ABSTRACT

SPATIAL AND TEMPORAL DEFORMATION PATTERN OF THE BRAIN FROM BLUNT TRAUMA

by

Abdus Ali

It is widely accepted that under extreme loadings the soft tissue of the brain will deform inside the skull, creating large amounts of both stress and strain on the tissue. This can result in a focal injury, or in the case of acceleration and deceleration, diffuse injuries. Any attempt at understanding the underlying mechanisms and effects of TBI, have to start by focusing on what is actually occurring within the brain. The objective of this experiment is to record differences in the spatial and temporal patterns of deformation within the brain during blunt trauma when changing impact parameters. A linear impactor is used to deliver controlled blows to the head surrogate, mimicking real-world blunt injury scenarios. Visual markers within head surrogates are used to motion track deformations and extract strains (principal tension, principal compression, max shear). The loading conditions include impact velocities at 3 and 5 miles per hour, impact locations at the crown of the skull and the forehead, and with the brain composition being either a 10% or 20% ballistics gelatin. To generalize, crown injuries cause higher strains than front impacts, and 5mph impacts cause larger strains than 3mph impacts. The 10% gelatin produce larger strain than 20% gelatin, but with large standard deviations. Contour maps of the maximum strains occurring in the brain reveal regional differences when comparing crown and front impacts at the mid sagittal plane. The results suggest differences in loading conditions cause heterogeneity in trauma outcomes.

SPATIAL AND TEMPORAL DEFORMATION PATTERN OF THE BRAIN
FROM BLUNT TRAUMA

by
Abdus Ali

A Thesis
Submitted to the Faculty of
New Jersey Institute of Technology
in Partial Fulfillment of the Requirements for the Degree of
Master of Science in Biomedical Engineering

Department of Biomedical Engineering

May 2017

Blank Page

APPROVAL PAGE

SPATIAL AND TEMPORAL DEFORMATION PATTERN OF THE BRAIN FROM BLUNT TRAUMA

Abdus Ali

_____

Dr. Bryan J. Pfister, Thesis Advisor   Date
Associate Professor of Biomedical Engineering, NJIT

_____

Dr. Namas Chandra, Committee Member   Date
Associate Professor of Biomedical Engineering, NJIT

_____

Dr. Maciej Skotak, Committee Member   Date
Associate Research Professor of Biomedical Engineering, NJIT

BIOGRAPHICAL SKETCH

Author: Abdus Ali

Degree: Master of Science

Date: May 2017

Undergraduate and Graduate Education:

- Master of Science in Biomedical Engineering,
  New Jersey Institute of Technology, Newark, NJ, 2017

- Bachelor of Science in Biomedical Engineering,
  New Jersey Institute of Technology, Newark, NJ, 2016

Major: Biomedical Engineering

Presentations and Publications:

Ali, Abdus et al. (2017, April). *The Effects of Blunt Impact Site and Speed on the Spatial and Temporal Deformation of the Brain* Poster presented at the annual Northeast Bioengineering Conference, Newark, NJ

Ali, Abdus et al. (2016, December). *Spatial and temporal deformation pattern of the brain from blunt trauma* Poster presented at the annual Rutgers Brain Health Institute Symposium, Branchburg, NJ

Swenson, Brian et al. (2016, October). *Spatial and temporal deformation pattern of the brain from blunt trauma* Oral presentation at the Biomedical Engineering Society Annual Meeting, Minneapolis, MN

This thesis is dedicated to my family and friends. Their support and influence

(deliberate and accidental) is why I made it this far.

ACKNOWLEDGEMENT

TABLE OF CONTENTS

Chapter	Page

LIST OF TABLES

LIST OF FIGURES

LIST OF SYMBOLS AND ABBREVIATIONS

ε_1 Principal tensile strain

ε_2 Principal compressive strain

γ_{max} Max shear strain

LIST OF DEFINITIONS

AIS Injury Scale   Reports threat to life using injury type, location, severity

Coup contrecoup injury   Injury on the site of impact (coup) and the opposite side (contrecoup)

Glasgow Coma Scale   Scale used to classify TBI and mild, moderate, or severe based on eye, verbal, and motor response

CHAPTER 1

INTRODUCTION

1.1 Introduction to Traumatic Brain Injury

A traumatic brain injury (TBI) refers to any brain dysfunction caused by an external force on the head. TBIs account for approximately 30% of injury deaths worldwide and accounted for 2.8 million emergency room visits, hospital visits and death in the United States in 2013 [1]. Figure 1.1 breaks down the leading causes of TBI in the United States, all of which could include blunt contact force as a component of the injury. Figure 1.2 illustrates the distribution of these causes of TBI amongst different age groups [2]. In addition to the civilian population, TBIs are a concern for among military personnel. 361,092 TBIs were reported from 2000-2016 amongst American soldiers deployed worldwide [3]. Figure 1.3 delineates the distribution in injury severity for solders in 2016. Of note is the fact that more than 80% of the TBIs are mild [4]. It is clear that TBIs occur to a large population and is worth understanding, both to effectively prevent and efficiently treat patients in the future.
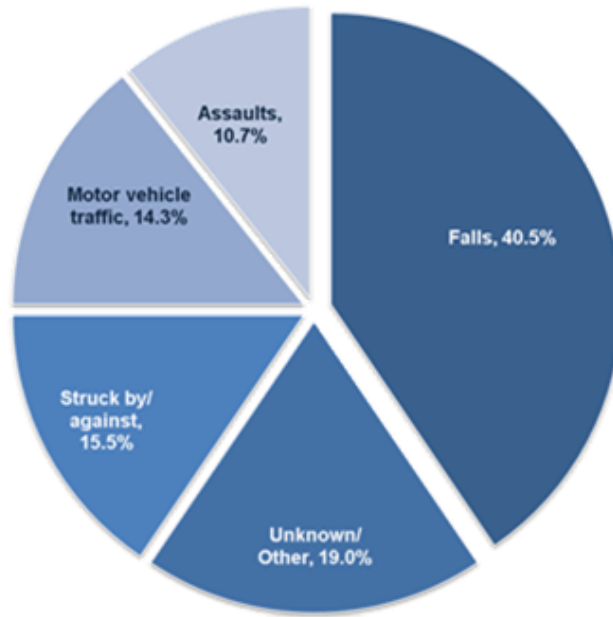
Figure 1.1 Leading Causes of TBI
Source: [1]
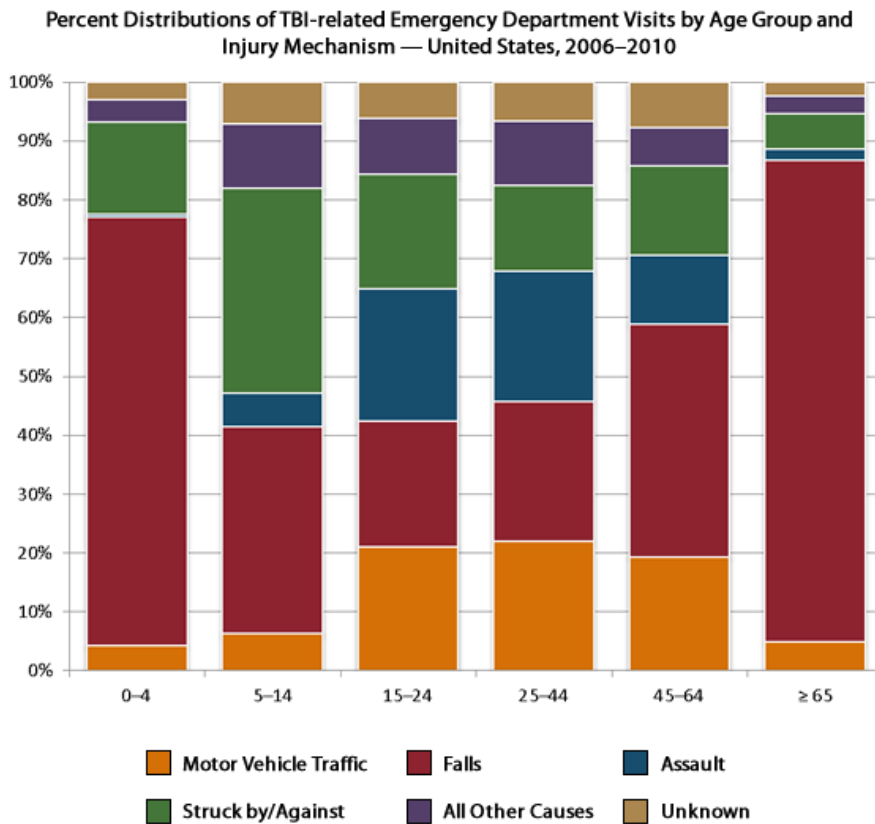
Figure 1.2 Percent Distribution of TBI-related Emergency Department Visits by Age Group and Injury Mechanism - United States, 2006-2010
Source: [2]

Figure 1.3 DoD Numbers for Traumatic Brain Injury Worldwide – Totals in 2016
Source: [4]

1.2   Mechanics of TBI

Blunt, blast, penetrating, and rotational injuries can be considered to be the major mechanical instigators for TBI. The mechanical behavior and clinical outcomes differ depending on the injury mode. Understanding the effects of each injury mode is outside the scope of this work, but the focus will be on blunt injuries. Blunt injuries refer to injuries caused by an external force coming in contact with the head.

A cross section of the various components that make up a human head would show skin, skull, cerebrospinal fluid (CSF), the meningeal layers, vasculature, and the white and grey matter of the brain, all of which make unique contributions to the mechanical outcome during a blunt impact. Other parameters such as the force, material hardness of the

impactor, contact area on the head, contact duration, location of impact, impact velocity, age of subject, weight of subject, and gender of subject also contribute to the injury outcome.

Understanding the role of each contributor is difficult due to the sheer amount of information that needs to be considered. For example, the skull size and its properties are variable. Highly interlinked sections of cranial sutures have been observed to absorb twice as much energy as cranial bone before fracture [5]. Cranial bone thickness is not uniform, with occipital bone typically being the thickest region, men having thicker skulls on average, and with thickness changing with age [6,7]. When comparing peak forces experienced by the bone before fracture, the occipital region is able to withstand the largest force, and the lateral regions the least [8].

The outcome of the injury [9] may be either a closed head injury or an open head injury. Closed head injuries refer to when the skull remains intact. Contusions, or bruising, may still occur as well as brain swelling which lead to increased intracranial and interventricular pressure (ICP, IVP) and more secondary injuries. Open head injury refers to when the skull fractures. It may be a hairline fracture, a depressive fracture where the broken piece moves towards the brain, or a compound fracture when the skull breaks into several pieces and cuts into the scalp. Blunt injuries are typically focal injuries, meaning that the site of impact is where the injury is worst, with little immediate effect on the rest of the head. However, if the impacting energy is high enough, there will be a coup-contrecoup injury, meaning that the energy from the impact was high enough to cause the brain to bruise at the site of injury as well as deform on the opposite side of the head and injure it as well. It is important to note that no mechanical instigator typically acts alone in

real-world scenarios. For example, a motor vehicle crash (MVC) may have a blunt and a rotational component, from the contact between a head and the car's interior (blunt) and from the rapid deceleration of the vehicle from several miles per hour to zero during impact (rotational).

1.5 Injury Criteria and Thresholds

Injury severity scales serve the purpose of helping medical personnel treat patients, as well and making it easier to consolidate and compare data. TBIs are typically classified as mild, moderate, or severe. Various injury criteria exist for assessing tolerances when dealing with scenarios that result in TBI. Criteria include structural imaging, loss of consciousness, post-traumatic amnesia, Glasgow Coma Scale (GCS), and Abbreviated Injury Scale score (AIS).

Of note is the Head Injury Criterion (HIC), which is currently used by the National Highway Traffic Safety Administration (NHTSA) in rating vehicle safety [10]. HIC is defined as

$$HIC = \left\{ \left[\frac{1}{t_2 - t_1} \int_{t_1}^{t_2} a(t)dt \right]^{2.5} (t_2 - t_1) \right\}_{max} \tag{1.1}$$

where a(t) is linear acceleration in acceleration of gravity = 9.8 m/s^2 (g's) and t_1 and t_2 are the start and end times for a duration which generates the highest HIC value, or a set duration, typically 15 or 36ms. The HIC score is associated with an injury risk curve for skull fracture, the Wayne State Tolerance Curve (WSTC), from which thresholds were initially generated. Animal, cadaveric, finite element model, and dummy data have been used to update the values for upper safety limits. It has also been used to study sports concussions and the effectiveness of protective gear. HIC is useful in its application in preventing severe head injuries, but several criteria exist which take into account more than

linear acceleration. For example, Brain Injury Criterion [11] (BrIC) has been proposed as a complement to HIC to account for the directional dependence of injury risk:

$$BrIC = \sqrt{\left(\frac{w_x}{w_{xC}}\right)^2 + \left(\frac{w_y}{w_{yC}}\right)^2 + \left(\frac{w_z}{w_{zC}}\right)^2} \qquad (1.2)$$

where w_x, w_y, and w_z are maximum angular velocities about the x,y, and z axes respectively and w_{xC}, w_{yC}, and w_{zC} are experimentally found critical angular velocities.

Experimental and computational data on strain thresholds are available in Table 1.1, as are results from impact studies in Table 1.2. What these tables highlight are the wide variety of methodology and reported measures. Reported values include peak pressure, linear acceleration, angular acceleration, and angular velocity, as well as more clinically used measures such as skull fracture, brain lesion, HIC score, and AIS injury scale score. The benefit of a good head surrogate is that it can be designed to be used in the majority of the experiments described in said tables, and are repeatable at any equipped facility.

Table 1.1 Strain Thresholds

Source: [12]

Study	Injury type	Injury criterion	Stated tolerance level in % strain	Method
Bain and Meaney (2000)	Severe criterion	Strain to cause functional impairment	13	dynamic stretching of the right optic nerve of an adult male guinea pig
	Optimal criterion		18	
	Liberal criterion		28	
	Severe criterion	Strain to cause morphological damage	14	
	Optimal criterion		21	
	Liberal criterion		34	
Morrison III et al. (2003)	Injury to hippocampal slice cultures	Strain	> 10	Dynamic loading on hippocampal slice cultures
Ellis et al. (1995)	injury of astrocytes	Strain	31 - mild, 38 - moderate, 51 - severe	Dynamic loading on astrocyte cell cultures to evaluate injury of astrocytes
Deck et al. (2008)	50% probability of mild brain injury	First principal strain	31	finite element reconstruction of motor sports, vehicle, football and pedestrian accidents
	50% probability of severe brain injury		40	
Kleiven (2007)	50% probability of concussion	First principal strain (corpus callosum)	21	Finite element reconstruction of football collisions
		First principal strain (gray matter)	26	
Margulies et al. (1992)	Moderate to severe DAI/brain injury	Strain	5 - 10	Experimental study on baboon (monkey), physical model and analytical simulation
Stalnaker and Mcelhaney (1970)	Severe brain injury	Maximum strain	0.329	Experiments on human cadaver skull and mathematical analog of skull-brain system

Table 1.2 Experimental Impact TBI

Source: [12]

Author and year	Study description	Input conditions	Reported head kinematics	Reported ICP values	Main findings
Nahum et al. (1976)	Impact tests on 10 seated cadavers. The cadavers were impacted with impactors of varying masses (5.18 to 5.38 kg) and varying velocities (3.56 to 9.6 m/s).	Peak force : 2.9 to 12 kN, Durations: 3-18 ms impact velocities: 3.6 to 9.6 m/s	Resultant linear acceleration : 44 to 327 G		Lesions type injuries were produced at linear accelerations of 195 G or more.
Nahum et al. (1977)	Impact tests on 8 seated cadavers. The cadavers were impacted with impactors of varying masses (5.23 to 23.09 kg) and varying velocities (4.36 to 12.95 m/s).	Peak force : 5.2 to 14.8 kN, impact velocities : 8.4 to 13 m/s	resultant linear acceleration : 155 to 433 G	Peak pressures Frontal: 427 kPa. Parietal: 9 to 221 kPa, and posterior fossa: -65 to -3 kPa.	Comparison of measured ICP and acceleration values with injury severity (as determined from pathologic examination) indices such as GSI and HIC resulted in reasonable correlation but scatter in the data was huge. It was determined that more data points were needed to establish clear relation with any measures and hence severity of injury
Stalnaker et al. (1977)	Impact tests on 15 cadavers seated upright. Cylindrical impactor of diameter 152 mm and mass 10 kg and was used to deliver an impact.	Peak force : 4.2 to 14.6 kN, Durations: 3.2 and 10.6 ms	resultant linear acceleration : 125 to 532 G, peak angular velocities : 12 to 44 rad/s, and peak angular acceleration: 5.5 and 37.6 krad/s2	140 kPa	General agreement between load severity and degree of injury was found but specific correlations could not be identified due to scatter among a small number of samples. Pressurized heads shown improved coupling between the skull and the brain, suggesting that relative motion between the brain and skull is minimized in vivo.
Nusholtz et al. (1984)	Impact tests on 9 cadavers. Cylindrical impactors of diameter 150 mm and mass of either 25 or 65 kg	Peak force : 0.8 to 10.2 kN, Durations: 8 to > 50 ms, impact velocities : 3.6 to 5.7 m/s	resultant linear acceleration : 25 and 459 G, peak angular velocities : 18 to 52 rad/s, and peak angular	180 kPa in the frontal region and -62 kPa occipital region	While no measured parameters correlated perfectly with injury severity, resultant linear and angular accelerations were the most predictive. Injuries were produced for translational head accelerations

	were used to deliver an impact.		acceleration: 0.8 and 42 krad/s2		>161 G or rotational head accelerations >7.2 krad/s2
Trosseille et al. (1992)	Impact tests on 2 cadavers.	Impactor velocity : 5-7 m/s			No injuries were reported as a result for linear and angular accelerations < 60 G and <4.3 krad/s2 and a minimum occipital pressure of —30 kPa.
Walsh et al. (1985)	Lateral impacts in 18 cadavers simulating pedestrian contact by an automobile. Some cadavers were also directly impacted by 23.5 kg impactor.	Impactor velocity : 4 m/s	Peak linear accelerations : 60 to 280 G		No correlation between HIC and injury (as coded by AIS) could be found.
Mcintosh et al. (1993)	Impact tests on 17 cadavers seated upright. Cylindrical impactors of diameter 150 mm and mass 25-28 kgs were used to deliver an impact.	Impactor velocity : 2.8 to 6.1 m/s			It was estimated that moderate brain injuries can be expected at resultant linear accelerations of 200 G.
Rizzetti et al. (1997)	Impact tests on 14 cadavers with impactor of mass 23 kg and diameter 150 mm.	Peak force : 3.6 to 20 kN, Impactor velocity : 5.3 to 5.8 m/s	Peak linear accelerations: 70 to 92 G for padded impacts and from 130 to 160 G for unpadded impacts.	Contre coup pressures: -20 to -46 kPa	Injuries produced suggest that linear acceleration was more relevant as a severity predictor than rotational acceleration.
Got et al. (1978)	42 free fall tests on fresh cadavers from heights of 1.83, 2.5, and 3 m	Impact force was measured but it was found unreliable.			It was also reported here that there was a minor chance of injury when HIC < 1500. Nahum et al. reported severe injuries with a HIC value as low as 657, indicating the enormous variability in reported values depending on the how the input load is imparted to the specimen, specimen condition and specimen preparation.

Hardy et al. (2001,2007)	Impact tests on cadavers. A 152-mm diameter impactor with impact velocities ranging from 2 to 4 m/s was used to impact the occipital region.	Impactor velocity < 4 m/s	peak linear acceleration : 12- 108 G, and peak angular acceleration: 2.5 and 7.5 krad/s2		Study mainly focused on understanding relative motion between the skull and the brain.

10

1.6 Research Aims

The objective of this study is to understand the effect of blunt impact loading parameters on the deformation field in the brain. Specifically, this study aims to:

Build on previous work on a head model for studying the deformation field following blunt impacts

Improve the experimental setup to lessen the effect of glare

Utilize the full marker grid within the head models in analysis

Calculate principal strains and associated strain rates from marker grid

Evaluate the effects of changing impact velocity between 3 and 5 mph and impact orientation between crown and front injuries

Identify model limitations and potential future directions for surrogate head models

CHAPTER 2

METHODS

2.1 Design of Head Model

2.1.1 Skull

To mimic the human skull, geometrically accurate 1:1 scale PVC skulls were used from Anatomy Warehouse. In order to visualize the impact and understand the deformations occurring at different sections of the head, the portions of the skulls had to be excised. The skull was cut along a 2cm offset from the midsagittal line to mimic a ½ skull (Figure 2.1). At the point of purchase, the skull was already separated into 3 pieces (skullcap, base of skull, and jaw) and had several 2mm holes for joining its pieces. The jaw was removed because it lacked relevance to the experiments being done. After making the desired sagittal cut, the two pieces of the skull (cap and base) were permanently fixed and the holes were filled using a combination of hot glue and epoxy.

2.1.2 Brain Fabrication and Marker Placements

The brain was mimicked using 10% and 20% ballistics gelatin melted and poured into the skull cavity, as depicted in Figure 2.2. The skull lacks a flat surface parallel to the midsagittal line, which makes it difficult to make a level pour of ballistic gelatin into it. An adjustable base was made to solve this issue. By moving nuts along bolts, the angle of the base could be adjusted. The skull was fixed with tape to the protruding bolts. This adjustable base was placed into a large pot. The appropriate ballistics gel was melted as per manufacturer's instruction. The protrusions on the internal surfaces of the ethmoid bone and occipital bone were estimated to be as the plane where midsagittal line would fall, and ballistic gel was poured to that point. The lid of the vacuum was placed, and the vacuum

was turned on for approximately 10 seconds and then the motor was shut off. After approximately 90 seconds, the vacuum was released, allowing air back into the chamber. Any remaining bubbles were manually dragged to the edge of the skull surface and popped. To help remove remaining bubbles, having the ballistics gel remain liquid would give it more time to come to the gel surface and pop. To accomplish this, the lid of the chamber was put on again to retain heat, without turning on the vacuum. The gel was allowed to solidify for at least 8 hours.

A 3D printed grid of holes was used to create a marker array on the surface of the brain surrogate. The purpose of this grid of markers was to be able to be captured by a high-speed camera and motion tracked. The grid separated the centers of each marker by 0.375mm. The printed grid was cut to fit into the inside of the skull and onto the surface of the gel. With the grid laying on the gel, black acrylic spray paint was used to form markers on the gel surface. The paint was allowed to dry for at least 4 hours. Once the paint had dried the skull was filled to the cut surface of the skull.

2.1.3 Miscellaneous Parts and Assembly

A ¼ inch thick sheet of polycarbonate was cut to fit onto the surface of the skull and create a viewing window. A lubricant, WD40, was placed on the gel and polycarbonate surfaces to allow for motion between the two materials with minimal friction. The window was attached to the skull using a clear epoxy and silicone.

To attach the completed head to the Hybrid III neck, and interface between the two had to be made. A ½ inch sheet of polycarbonate was cut to the shape of the metal plate on the hybrid III and holes were made at the same places the metal sheet already had. The bottom of the skull surface, where the foramen magnum is, was attached to the surface of

the polycarbonate sheet using double sided tape (3M automotive) and hot glue. The neck and head assembly attached to the linear impactor using custom shop-made mounting devices. One of the custom-made bases allowed for the head assembly to be placed onto the linear impactor at a 45 degree angle. The other base allowed for the assembly to be attached flat onto to the impactor base surface.
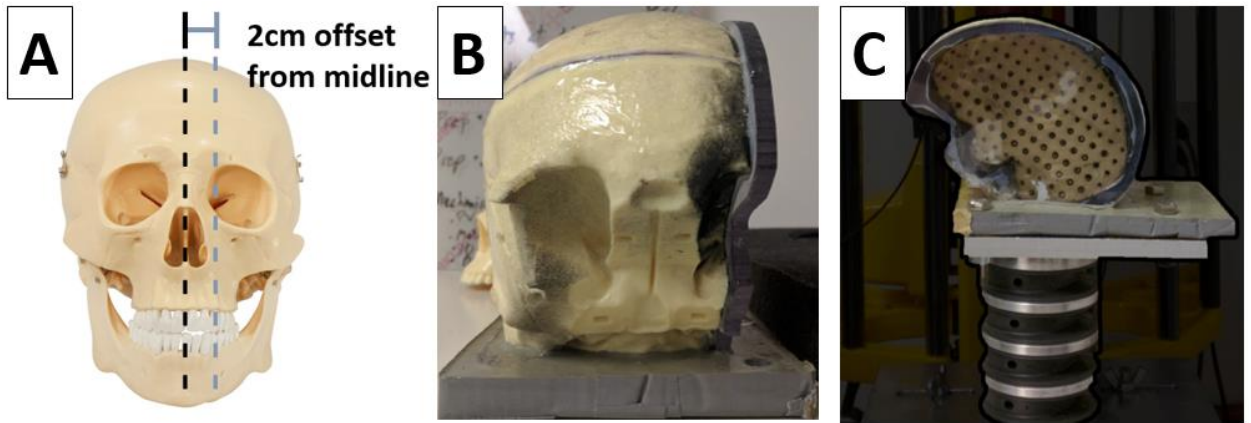
Figure 2.1 Head model components

A. Originally purchased PVC skull with demarcation on midline in black, and the 2cm offset used to cut the model.

B. Coronal view of the head model. Visible are the sagittal cut on the skull, fixation of skullcap onto base, polycarbonate window, and epoxy interface to neck.

C. Sagittal view of head model: the PVC skull, 20% ballistic gelatin brain with the marker grid, polycarbonate viewing window, epoxy base, and Hybrid III anthropomorphic neck.
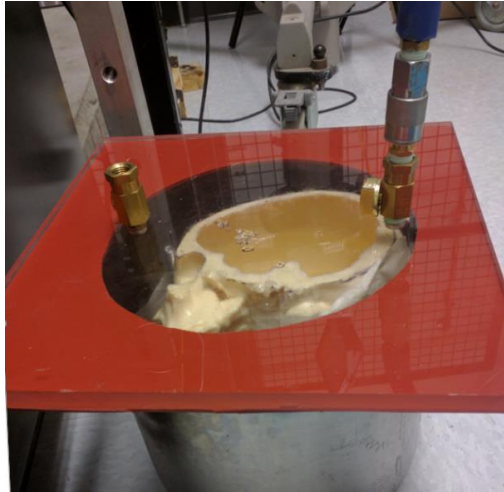
Figure 2.2 Production of ballistic gelatin brains

Note: Head model is placed inside a metal pot, with a polycarbonate sheet with a ring of silicone(red) to seal the edges. The protrusion on the right side of the surface connects a tube to a vacuum to remove air from the container, pulling out bubbles.

2.2 Drop Tower Test

To simulate real-world injury scenarios, the completed head model was used in conjunction with a linear impactor, as shown in Figure 2.3. The linear impactor machine, manufactured by Cadex Inc of Canada, is a Uniaxial Impact Monorail Machine (1000_00_MIMA). It is outfitted with a uniaxial accelerometer in the impactor in order to calculate impact acceleration and HIC. It is also equipped with a time gate to allow for impact velocity to be measured. The drop height is the input variable for the drop tower, with increased drop heights corresponding to increased impact velocities. In this case, the head model was placed on top of the surface with the load cell and struck by the impactor at 3 and 5mph.

For the purpose of this experiment, three parameters were varied for the experiments: drop height (velocity), impact location and gel concentration. Table 2.1 outlines the different values used for these parameters. Each possible combination of

variables, for example a 3 MPH impact on the forehead of the 10% gel skull, was run for

six trials (drops). This resulted in a total of 48 drops (8 combinations at 6 trials each).
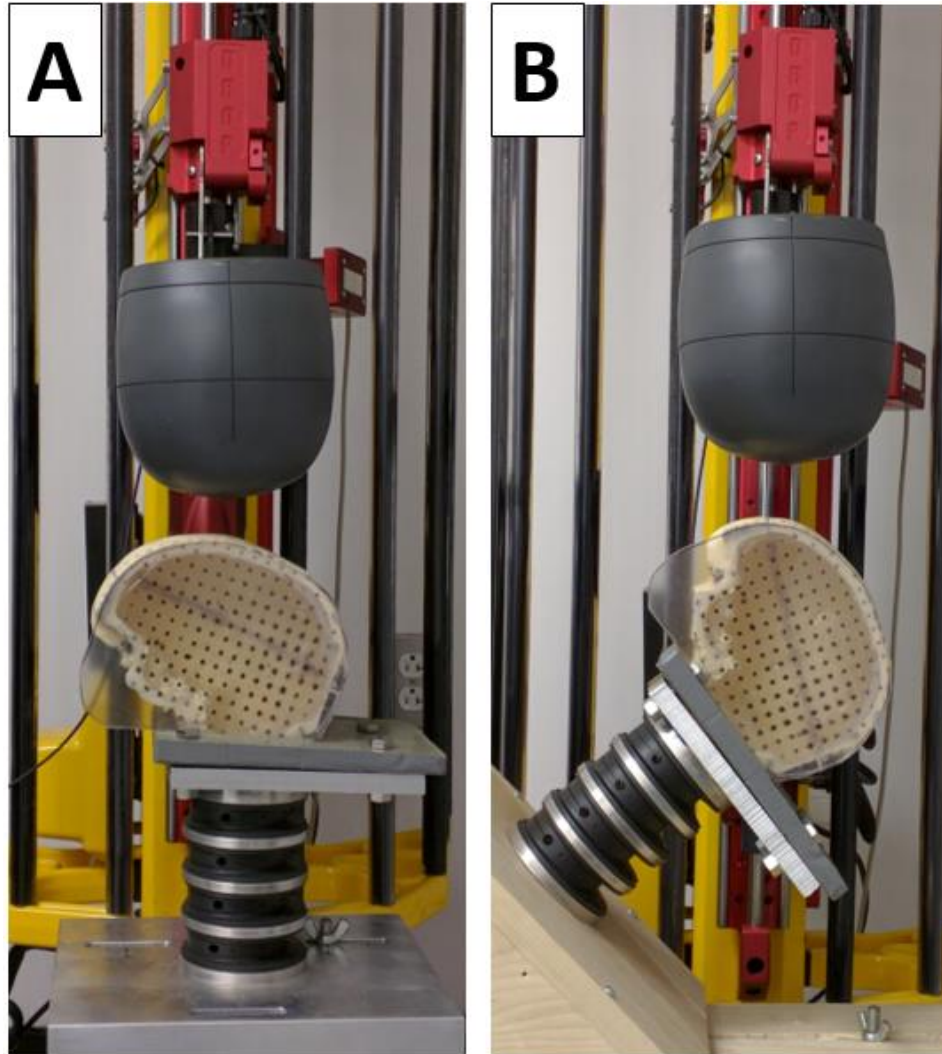
Figure 2.3 Blunt impact experimental setup. The head model is sitting on such that the linear impactor (grey) will contact the skull at either the (A) crown, or (B) front.

Table 2.1 Summary of Experimental Parameters

Parameter	Value 1	Value 2
Drop Height (Velocity)	9 cm (3 MPH)	25 cm (5 MPH)
Gel Concentration	10%	20%
Impact Location	Forehead	Crown

2.3   High Speed Video Imaging System and Light Control

The various injury events were captured using a high speed camera (UX100 M3 camera by Photron, USA) recording at 1000 fps. The camera was set to be facing perpendicular to the surface of the viewing window, ensuring that the viewing angle would not cause a distorted view of the motion of the markers.

High speed photography requires a relatively large amount of light in order to capture details. Though obvious solution would be to increase light, glare would be generated by reflecting off of the head model's viewing window as well as the ballistic gel during deformations. This would make marker tracked data unusable if the glare persisted for several frames of the video. Two external LED lights were aimed at the head model at various angles in order to minimize the amount of glare present.

2.4   3D Kinematic Reconstruction and Data Acquisition

The motions of a selected grid of black markers were captured using ProAnalyst's 2D tracking feature. For each video, brightness and contrast were adjusted to help the motion tracking algorithm's accuracy. All resulting motion-tracked data was inspected visually to

correct for tracking errors the software may have made. The data was also checked with a custom MATLAB script for the locations (marker number, frame number) of unusually high deformation values which would then be checked again in the Pro Analyst software manually.

The 2D tracked marker data was exported from ProAnalyst as marker numbers and its respective location in an arbitrary but consistent coordinate system over time in excel spreadsheets. These spreadsheets were loaded into MATLAB. A custom algorithm was written to analyze the data (Appendix A). Due to degradation of the markers after repeated use, the number of usable markers were inconsistent between the 10% and 20% ballistic gel models. For the 10% and 20% gels, 90 markers and 126 markers were used in the analysis respectively.

2.5   Calculation of Strain Tensor, Principal Strain, and Strain Rate

Continuum theory can be used to explain what occurs to the head during a blunt impact. The kinematics can be described using discrete units, in this case a motion tracked grid of markers, to describe a continuous mass, in this case a homogenous brain made out of ballistics gelatin. The undeformed state refers to the head model before impact. When an external force contacts the head, rigid body movement will occur. Each frame post-impact can be considered in the analysis as a deformed state. In addition, there is relative motion between the skull and brain, with deformation of the brain as well.

For each impact, principal tensile strains, principal compressive strains, and maximum shear strains were found. Their associated strain rates, and locations within the marker grid were also recorded.

Sets of 4 points from the marker grid were used to form squares, as displayed in Figure 2.3A. For each square, perpendicular vectors were created using an origin point, the adjacent right point, and adjacent lower point. The two vectors, dXh and dXp were set using the first frame of the video, as displayed in Figure 2B, as the undeformed state. For later frames, these two vectors became dxh and dxp respectively, representing the deformed state.
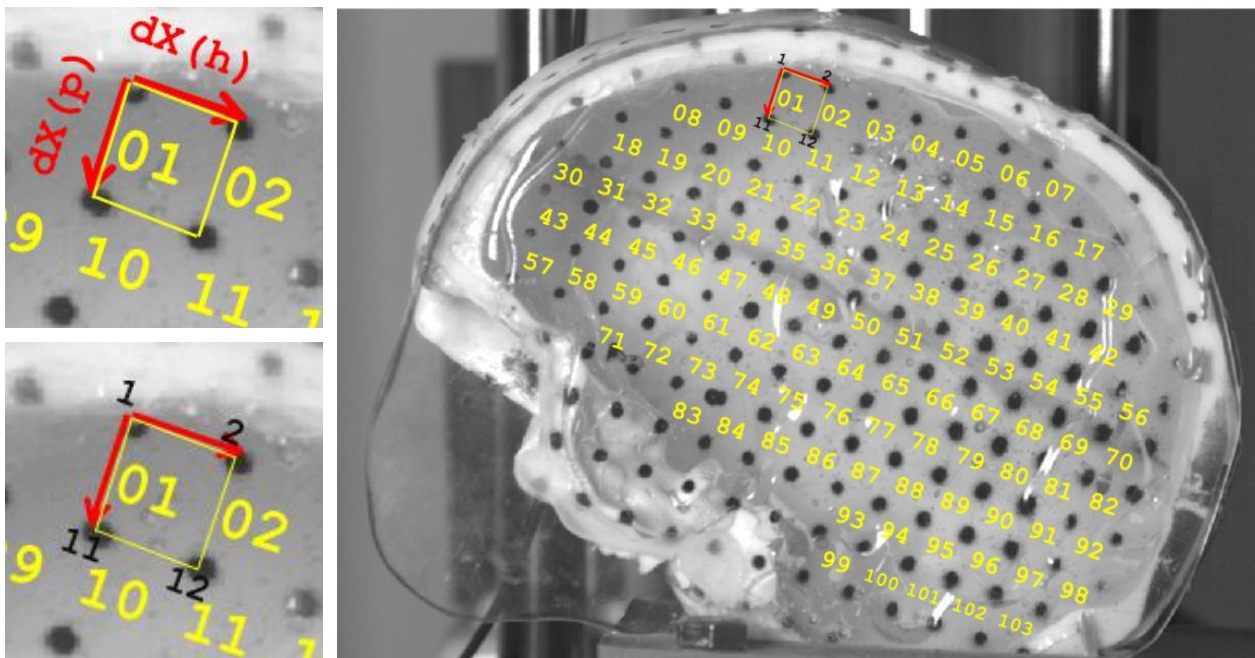
Figure 2.4 Transforming markers into motion-tracked deformation grid
(A) This figure indicates the numbering of the squares and the formation of deformation gradient tensor. The yellow numbers indicate square formed by the surrounding black markers. The two vectors created, $dx^{(h)}$ and $dx^{(p)}$, which the deformation gradient and strain tensor was created indicating the strain information of 1 of several squares within the grid.

(B) The 4 black numbers indicate user-defined markers set at the location of black dots, which are motion tracked

(C) 103 squares within the marker grid, indicating the spatial locations for each of the set of strain calculations

Using the two vectors, the deformation gradient F, which is a series of 4D matrix including the information of deformation along x direction, y direction and shear deformation within each square was calculated using Eq 2.1 and Eq 2.2. Then, The Cauchy-

Green tensor C was used to eliminate the rotation effects caused by the neck flexion using Eq 2.3. The Lagrangian strain tensor E was found using Eq 2.4 and 2.5. From these values, it was converted into the principal strains, with principal tensile strain ε_1 in Eq 2.6, principal compressive strain ε_2 in Eq 2.7 and maximum shear strain γ_{max} in Eq 2.8.

$$[(dx^h)'(dx^p)'] = F[(dX^h)'(dX^p)'] \tag{2.1}$$

$$F = [(dx^h)^T(dx^p)^T] \times [(dX^h)^T(dX^p)^T]^{-1} \tag{2.2}$$

$$C = F^T \times F \tag{2.3}$$

$$E = (F^T \cdot F - I)/2 \tag{2.4}$$

$$E = \begin{bmatrix} \varepsilon_{xx} & \varepsilon_{xy} \\ \varepsilon_{yx} & \varepsilon_{yy} \end{bmatrix} \tag{2.5}$$

$$\varepsilon_1 = \frac{\varepsilon_{xx} + \varepsilon_{yy}}{2} + \sqrt{\left(\frac{\varepsilon_{xx} - \varepsilon_{yy}}{2}\right)^2 + \left(\frac{\varepsilon_{xy}}{2}\right)^2} \tag{2.6}$$

$$\varepsilon_2 = \frac{\varepsilon_{xx} - \varepsilon_{yy}}{2} - \sqrt{\left(\frac{\varepsilon_{xx} - \varepsilon_{yy}}{2}\right)^2 + \left(\frac{\varepsilon_{xy}}{2}\right)^2} \tag{2.7}$$

$$\frac{\gamma_{max}}{2} = \sqrt{\left(\frac{\varepsilon_{xx} - \varepsilon_{yy}}{2}\right)^2 + \left(\frac{\varepsilon_{xy}}{2}\right)^2} \tag{2.8}$$

Strain rates $\dot{\varepsilon}$ were calculated using the slope at the maximum strains associated with each location within the grid in Eq 2.9. To find the slope, the MATLAB script differentiated the strain time course (Fig 2.4) to find a millisecond by millisecond strain rate. Counting back from the point of max strain, it checked for all positive nonzero values within the same series. It then found the slope between the first positive point and the point of max strain as the strain rate.

$$\dot{\varepsilon} = \frac{\varepsilon_{MAX} - \varepsilon_{MIN}}{t_{MAX-MIN}} \tag{2.9}$$
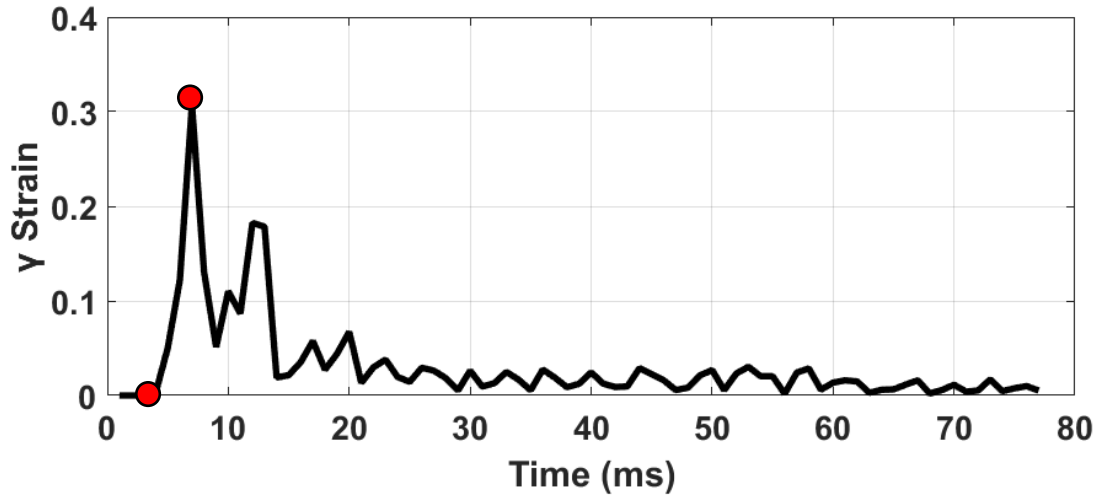
Figure 2.5 Representative shear strain time course from one location during an impact

Note: The red markers depict the two points used in calculating the strain rate, the first positive strain rate leading up to the max strain.

After calculating strain and associated strain rate, the linear relationship between the two values were assessed using Pearson's correlation (r). The maximum strain values for a given impact (series of x values) were correlated with its associated strain rates (series of y values). After calculating this value for n in each group, r was averaged.

$$r = \frac{n(\sum xy) - (\sum x)(\sum y)}{\sqrt{[n \sum x^2 - (\sum x)^2][\sum y^2 - (\sum y)^2]}} \qquad (2.10)$$

The Cadex drop tower sensors, the accelerometer in the impactor and the 3 equidistant force sensors on the load cell surface, recorded at 33kHz. The Cadex system automatically sorted the generated data to output the peak acceleration and force values reported in the results. The velocity at the point of impact was generated with another sensor, a time gate acting as a velocimeter, that the impactor passes just before impact.

CHAPTER 3

RESULTS AND DISCUSSION

Presentation of the data generated from the impact events were done using conventional methods such as tables, line graphs, and bar graphs. The use of a visible track-able marker grid within the head model allowed for a unique opportunity to view the regional differences in the brain during an impact event.

Figure 3.1 illustrates the differences in strain along the time course following impact for different regions of the brain on the same model. The time course for the same three locations are plotted for the crown and front impacts. The purpose of this figure is to show how the same location can undergo drastically different deformation under the same injury condition with only the site of impact changed. Fig 3.1 A and D, B and E, and C and F are the time courses of the same locations, but it is clear that the peak principal strain values, duration of increased strain, and number of oscillations are different. The duration of increased strain values higher in the crown impact. While these properties of the waveform were consistent, the nature of the waveform made is difficult to quantify the duration of increased strain. The oscillatory motions caused inconsistencies in which peak would produce the maximum strain values as well as making it difficult to set arbitrary thresholds for where to begin and end the time duration of the "pulse". To address this, the beginning of the positive slope leading to the maximum strain value (Figure 2.3) was used for the calculation of the associated strain rate at the maximum strain value.
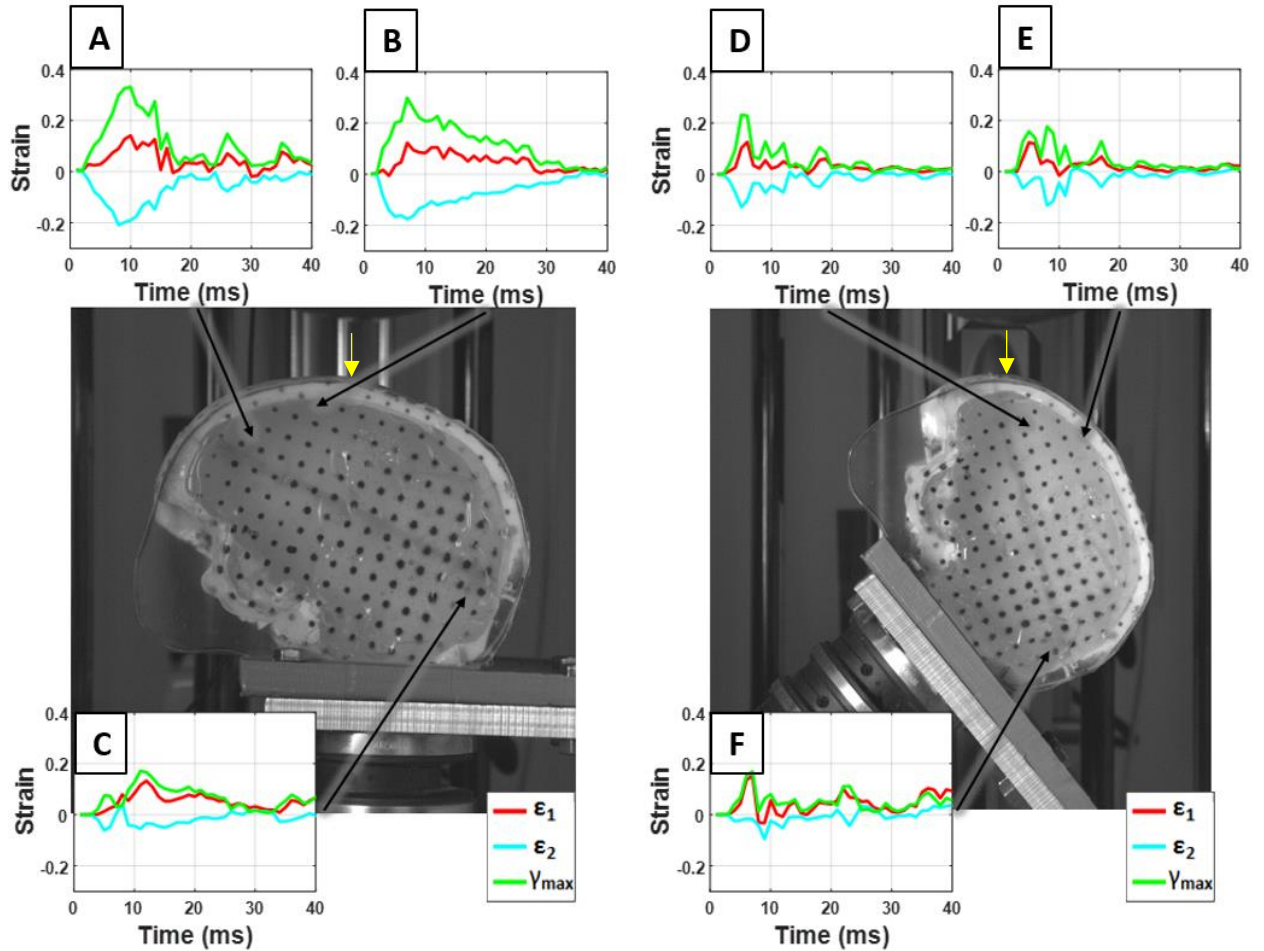
Figure 3.1 Comparison of strain-time courses at different locations of brain and at different impact sites with a 20% gel model during a 5mph impact

The left head model image represents a crown impact (A - C) and the right head model represents a front impact (D - F). Principal strains at selected markers were graphed to indicate the differences in their waveforms. Yellow arrows were superimposed on each image to show where the impactor contacted the skull surface.

Figure 3.2A illustrates that 5mph impacts cause higher strain values to occur than during 3mph impacts. Figure 3.2B shows crown impacts produced higher strain values to occur than front impacts. Crown and front tensile impacts produced average principal strains similar in value but still significantly different with $p<0.01$. In terms of principal compression and shear strains, crown impacts clearly produced higher deformations. Independent-samples t-tests were used to evaluate significance between populations. The

top 10% of strains (~10 values) were sampled, with 12 drops per parameter, with 2 parameters. This translated to 120 samples from each population, creating a large n and such significant differences despite overlapping standard deviation error bars.
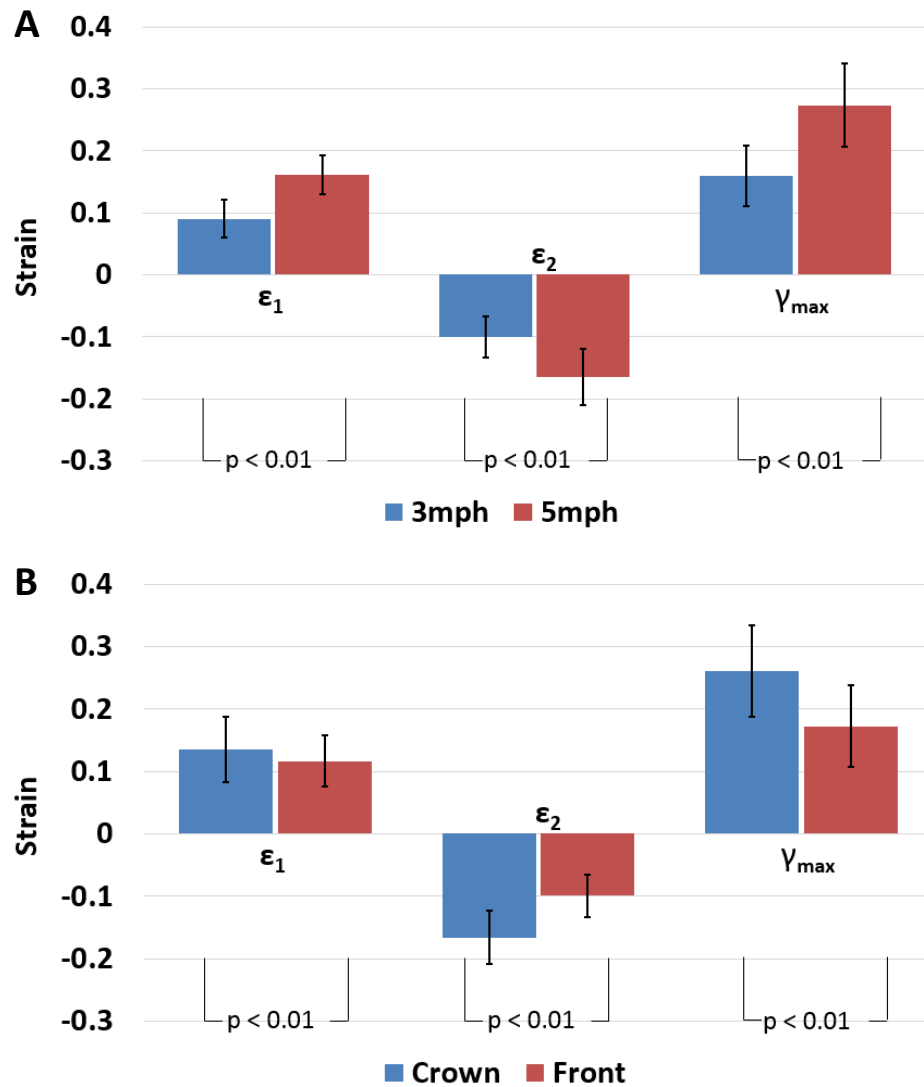
Figure 3.2 Effects of impact speed and impact orientation using the top 10% of strain values during impacts in 20% gel

(A) compares 3mph impacts to 5mph impacts. There are 12 total drops for each legend entry, with 6 crown and 6 front impacts for each

(B) compares crown impacts to front impacts. There are 12 total drops for each legend entry, with 6 3mph and 6 5mph impacts for each

ε_1 is principal tensile strain, ε_2 is principal compressive strain, and γ_{max} is the principal shear strain

Using the top 10% of strain values during impacts in the 10% gel generated unusually large standard deviations bars. Because of this, data for the 20% gel was presented for the remaining results. Possible causes of the inconsistency include a poorly formed boundary condition between the ballistic gel and window allowing for excessive movement, or an inherent property of a lower concentration ballistic gelatin.

The differences in strain distribution between the impact locations are illustrated in Figure 3.3. Despite changes in severity, the general "geography" of the heat-maps are similar between 3 and 5mph velocities. Data for 5mph impacts are only displayed because of this. The contour map matches the data seen in Figure 3.2, with larger strains occurring in crown impacts than in front impact. The localization of high strains are consistent with the impact sites, producing focal strains. It is of note that contrecoup strains were generated in the front impacts at 5mph during some experiments, but were ultimately averaged out. It is worth observing if this phenomenon becomes more pronounced at a faster impact velocity.
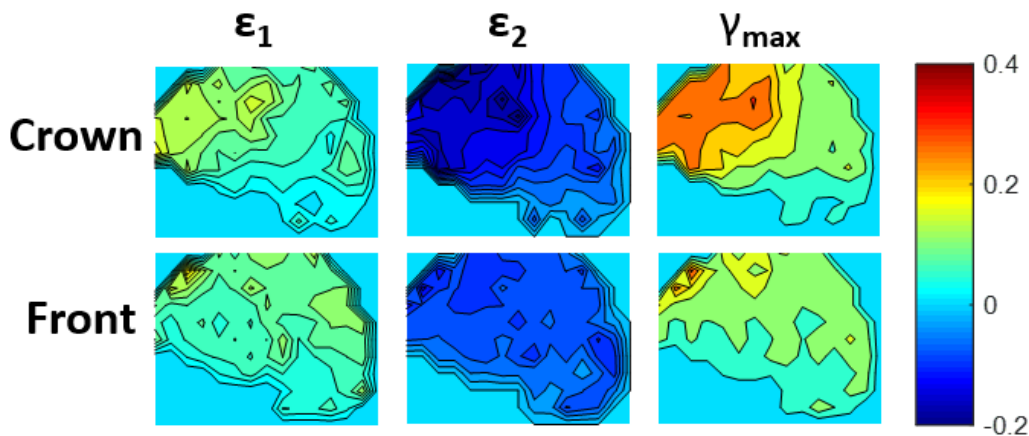
Figure 3.3 Contour maps of the three maximum principal strains in both impact orientations.

For each impact orientation (n=6 for each), the maximum strain value for at each data point was averaged and reconstructed on a contour map for 5mph impacts of 20% gel

Evaluating the maximum strain rates associated with the maximum strains have more relevance to the rest of the collected data, rather than finding the global maximum strain rate for a given location, as they may occur at two different times. This is presented in Figure 3.4. In literature, the rapid acceleration-deceleration that is referred to as causing injuries is evaluated as the global movement of the head (only measuring the skull's movement), or of discrete elements within the brain like in this study.
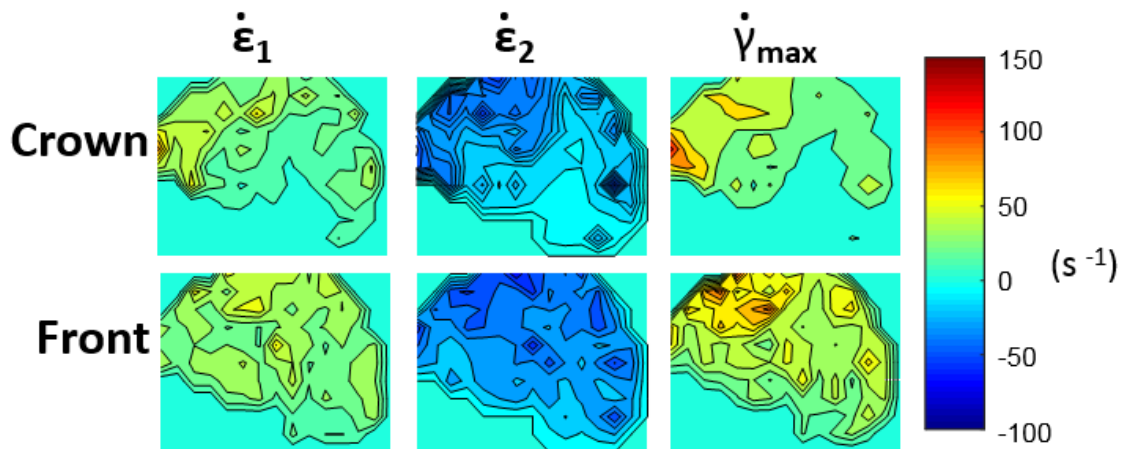
Figure 3.4 Contour maps of strain rates associated with maximum strain rates.
 For each impact orientation (n=6 for each), the strain rate was calculated at the maximum strain value for each data point and averaged using 5mph impacts of 20% gel.

The Cadex drop tower's time-gate interface, uniaxial accelerometer (in the impactor), and load cell (on bottom plate below neck) recorded data during impacts, found in Table 3.1, along with auto-generated calculations based on these recordings. NA refers to unavailable data which was missed due to user error in entering parameters into Cadex software or from glitches in the software itself. One entry for a 10% gel impact and two entries for 20% gel impacts are also unavailable. Figure 3.5 summarizes the most interesting information generated by the sensors. The crown impacts generated a peak acceleration of 20.4 ± 1.5 m/s^2 at 3mph and 36.4 ± 3.5 at 5mph, (n=11 for each speed; 10%

and 20% gel values were averaged together). The front impacts generated peak accelerations of 44.7 ± 5.1 m/s^2 at 3mph and 73.3 ± 7.0 m/s^2 at 5mph, (n=11 for each speed; 10% and 20% gel values were averaged together). The crown impacts generated peak forces of 1386.6 ± 46.8 N at 3mph and 2460.5 ± 182.2 N at 5mph, (n=8 for each speed; 10% and 20% gel values were averaged together). The front impacts generated peak forces of 582.8 ± 86.3 N at 3mph and 904.6 ± 197.2 N at 5mph, (n=8 for each speed; 10% and 20% gel values were averaged together). It is clear that the crown impacts generated larger forces on the load cell and front impacts caused larger peak accelerations on the impactor. It is important to differentiate that the data generated here helps to explain the motion of the head model but ultimately only describes what happened to the impactor and load cell, which are outside of the head model. Instrumentation of the head model would provide more insight to the injury severity generated by these experiments, and make these results' comparison to existing literature more accurate.

Table 3.1 Drop Tower-generated Data
Note: NA refers to unavailable data due to software and user error.

Gel %	Position	Velocity (m/s)	Peak Acc. (G) (m/sec^2)	Peak Force (N)
20	FRONT	1.2105	36.7	740
20	FRONT	1.1915	34.4	759
10	FRONT	1.2273	44.6	548.4
10	FRONT	1.2139	43.7	530.5
10	FRONT	1.2686	51.1	573
10	FRONT	1.2522	43.7	466.2
10	FRONT	1.485	49.7	623.7
10	FRONT	1.2273	41.8	543.7
20	FRONT	1.2099	48.3	549
20	FRONT	1.2044	49.2	527.8

20	FRONT	1.2208	47.9	549.1
20	FRONT	2.2041	60.9	1238.2
20	FRONT	2.2053	59.5	1275.1
10	FRONT	2.1874	77.1	653.6
10	FRONT	2.2153	76.7	657.4
10	FRONT	2.2994	79	678.8
20	FRONT	2.1807	80.8	897.2
20	FRONT	2.2038	80.8	908
20	FRONT	2.2391	76.7	950.5
10	FRONT	2.1971	71.5	872.3
10	FRONT	2.2108	72.5	890.4
10	FRONT	2.2599	70.2	929.3
20	CROWN	1.2217	18.6	1402.5
20	CROWN	1.2265	18.6	1403.9
10	CROWN	1.2288	21.4	1340.2
10	CROWN	1.2129	21.8	1355.7
10	CROWN	1.2032	21.8	1334.4
20	CROWN	1.3187	20.4	1492
20	CROWN	1.2066	19	1382.1
20	CROWN	1.1967	19.5	1382.2
10	CROWN	1.3611	22.3	NA
10	CROWN	1.2046	19.5	NA
10	CROWN	1.3922	23.2	NA
20	CROWN	1.2195	19	NA
20	CROWN	2.3599	33.5	2384.4
20	CROWN	2.2029	29.3	2165.1
10	CROWN	2.2986	42.7	2737.6
10	CROWN	2.1869	40.4	2644.1
10	CROWN	2.1772	39	2646.3
20	CROWN	2.2025	34.8	2406.4
20	CROWN	2.1521	34.4	2361.3
20	CROWN	2.1473	34.8	2339

10	CROWN	2.1902	35.3	NA
10	CROWN	2.1834	38.1	NA
20	CROWN	2.2082	38.1	NA

A

Peak Acceleration (m/s²)

B

Peak Force (N)
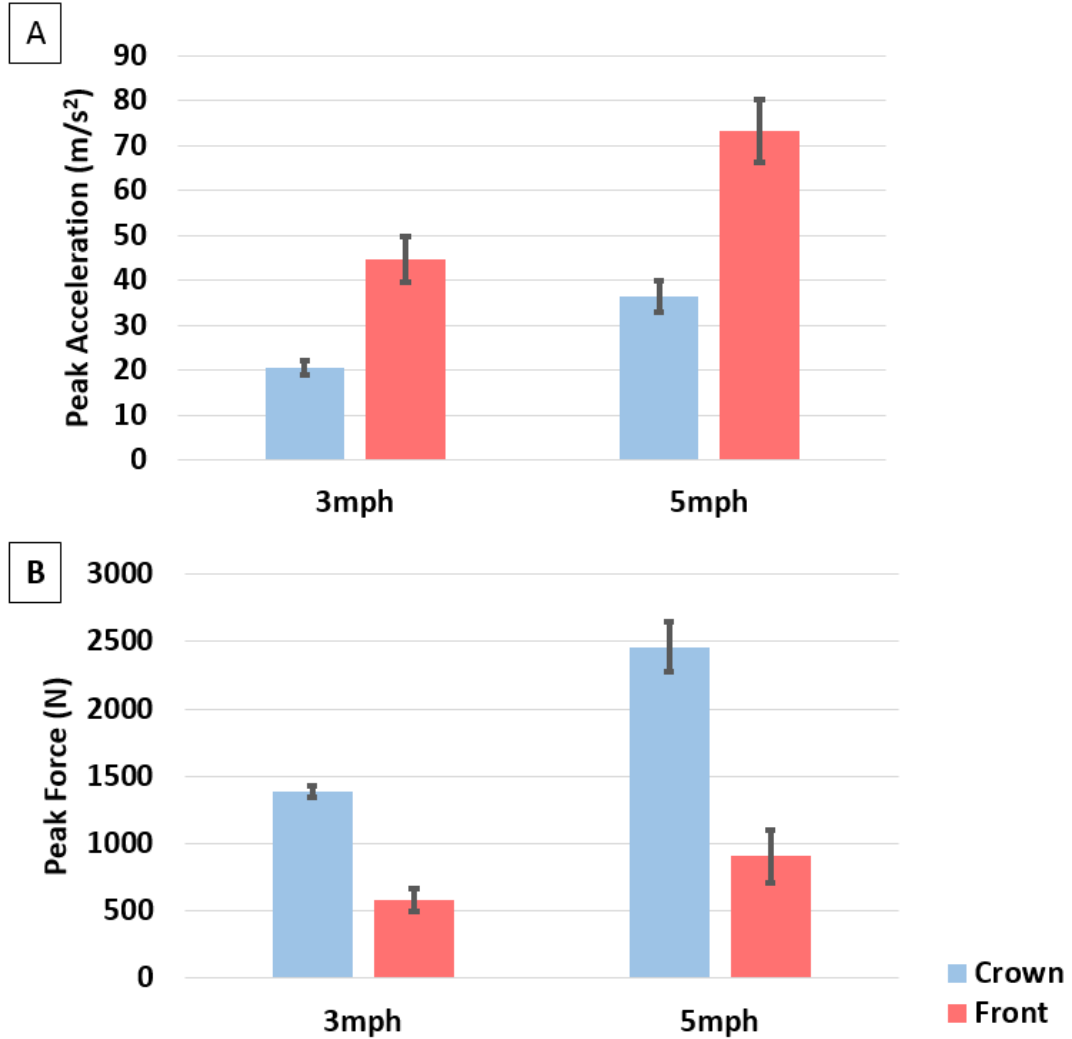
■ Crown
■ Front

Figure 3.5 Drop Tower sensor-generated data
(A) Comparison of peak acceleration in crown vs front impacts at 3 and 5mph.
(B) Comparison of peak in crown vs front impacts at 3 and 5mph.

Because the contour maps of strain and associated strain rates looked similar to each other in terms of contour lines between different regions, the correlation between said strain and strain rates were investigated. Pearson's correlation between the series of strain values in each individual drop and the series of strain rate values associated with those

strains were calculated, averaged, and tabulated in Table 3.2. For the 10% and 20% gel rows, n=12. For all other rows, n=6. Because there are different ways to combine the cases for the data, all possible options were used when averaging the cases to see the potential disparities in the correlations. The values do not exceed .64 (5mph 10%) for any group. Although no correlation is near 0, more meticulous control over experimental variables would be necessary to entertain the possibility that one of these observations about their relationships is worth further investigating.

Table 3.2 Correlation between the Series of Maximum Strain Values within the Deformation Grid in the Head Model and its Associated Strain Rates

	ε_1	ε_2	γ_{max}
10% gel	0.62	0.42	0.57
20% gel	0.52	0.49	0.59
crown 10%	0.66	0.39	0.56
crown 20%	0.57	0.52	0.60
front 10%	0.58	0.46	0.58
front 20%	0.47	0.45	0.58
3mph 10%	0.60	0.39	0.56
3mph 20%	0.51	0.47	0.60
5mph 10%	0.64	0.45	0.58
5mph 20%	0.52	0.50	0.59

CHAPTER 4

CONCLUSIONS AND FUTURE WORK

This thesis builds on previous work [13] using the same head models. Some questions mentioned in Miao 2016 remain unexplored. The effect of varying the impactor may be better in recreating real-world injury scenarios and inducing different, maybe characteristic-to-impactor, deformation patterns in the skull and brain. The brain simulants, 10% and 20% ballistic gel, have not been evaluated in comparison to softer, more "brain-like," materials which may be better suited for blunt impact experiments. While there were no observable differences in the distribution (not intensity) of strain in the brain between 3 and 5 mph, a faster impact may induce larger contrecoup strains.

The capability to measure skull deformation and marker acceleration and deceleration exist within this model but were not utilized due to time constraints. Placing markers on the cut surface of the skull would have added two important measures, skull deflection and the relative motion between the skull and brain. Understanding how much of the brain motions are due to the skull deforming would give insight into why certain populations are more or less affected by otherwise same injury events. It would be interesting to utilize in the case of a non-deforming vs deforming skull and visualize the differences in energy transfer. In the case of acceleration-based injuries such as MVCs, rupture of the bridging veins between the skull and brain are a major concern. The measurement of the relative motion would give insight as to how this model compares to real-world case studies and results from various experiments in literature.

A transparent skull is currently being developed. To solve current issues with glare due to limitations in lighting, a transparent skull allows for backlighting, meaning that there

should not be any reflected light captured on camera if used in an otherwise same model. Another potential benefit is the viewing of the brain surface during injury events. This would allow for tracking of the sulci and gyri of the brain as well as relative skull-brain displacement outside of the present single viewing plane.

The use of a purchased PVC skull made is easier to get geometric accuracy within the model, but may not be representative of how a real human skull would deform under the same impacts. The brain simulant in this model, 10% and 20% ballistics gel, have a significantly higher Young's Modulus than an actual human brain. Because of their relevance in blast, and ease-of-use, they were used for this model. The model lacked many of the internal structures present within the cranial cavity. These include the sulci, fissures, and ventricles of the brain, cerebrospinal fluid, the tentorium, and the meninges. Generating a model with more correct geometric and mechanical properties may give insight into more accurate deformation fields that would occur.

MATLAB CODE

The following MATLAB code was used to calculate strains, strain rates, and produce figures. Marked in green are notes meant to explain the purpose of a particular section or line to readers.

```matlab
clear all
dirdata00=dir('C:\Users\BlastLab\Desktop\Abdus\ChenStuff\10\*');dirdata
00=dirdata00(3:end);

for dir_num = 1
    clear oldbox outbox newbox
    tracking_reg=
xlsread(['C:\Users\BlastLab\Desktop\Abdus\ChenStuff\10\'
dirdata00(dir_num).name '\2Dtracking_inches.xlsx' ],'C24:FZ300');
%UPDATE

tracking_out=xlsread(['C:\Users\BlastLab\Desktop\Abdus\ChenStuff\10\'
dirdata00(dir_num).name '\additionaltracking.xlsx'],'C24:SZ300');
    quantity_old= size(tracking_reg,2)/2;  % #points in regular box
grid
    quantity_out= size(tracking_out,2)/2;  % #points outside regular
box grid

    clear points_box_old
    for i = 2:2:2*quantity_old
        points_reg(i/2,:,:)= tracking_reg(:,(i-1):i)';   % xy,#frames
    end
    clear points_box_out
    for i = 2:2:2*quantity_out
        points_out(i/2,:,:)= tracking_out(:,(i-1):i)';   % xy,#frames
    end

    points_all=vertcat(points_reg,points_out);
    frames=size(points_all,3);


    if size(points_reg,1)==70
        limit_points=121;

    else %size(points_reg,1)==92
        limit_points=20;
    end

    clear vectora vectorb undA invundA
    pointloc_vector_a_all=zeros(limit_points,2);
pointloc_vector_b_all=zeros(limit_points,2);
    for point_num_limited=1:limit_points % value limited to max for
vector b ...70pts -10pts in last row = 60pts
        clear dummy_matrix
        for point_num=1:size(points_all,1)
```

```matlab
dummy_matrix(point_num,:)=points_all(point_num_limited,:,1);
        end
        dummy_value_vector_a= points_all (0.45>abs(points_all(:,1,1)-
dummy_matrix(:,1)) & abs(points_all(:,1,1)-dummy_matrix(:,1))>0.1   &
0.1>abs(points_all(:,2,1)-dummy_matrix(:,2)));
        dummy_value_vector_b= points_all (0.45>abs(points_all(:,2,1)-
dummy_matrix(:,2)) & abs(points_all(:,2,1)-dummy_matrix(:,2))>0.3   &
0.1>abs(points_all(:,1,1)-dummy_matrix(:,1)));

pointloc_vector_a=find(points_all(:,:,1)==dummy_value_vector_a(end));

pointloc_vector_b=find(points_all(:,:,1)==dummy_value_vector_b(end));
        pointloc_vector_a_all(point_num_limited,:)=[point_num_limited
pointloc_vector_a];
        pointloc_vector_b_all(point_num_limited,:)=[point_num_limited
pointloc_vector_b];

        % Create perpendicular vectors a&b
        vectora(point_num_limited,:,:)=
points_all(pointloc_vector_a,:,:) - points_all(point_num_limited,:,:);
% Goes to end of 2nd to last row
        vectorb(point_num_limited,:,:)=
points_all(pointloc_vector_b,:,:) - points_all(point_num_limited,:,:);
% Goes to last point

        undA(:,:,point_num_limited)= [vectora(point_num_limited,:,1)'
vectorb(point_num_limited,:,1)'];    % Eq 3.4? from Chen's thesis
        invundA(:,:,point_num_limited)=
inv(undA(:,:,point_num_limited));
    end


    % Script for creating deformation gradient(F) and Lagrangian strain
tensor(E)
    clear Fa Ea
    for point_num_limited=1:limit_points
        for frame_num = 1:frames
            Fa(:,:,point_num_limited,frame_num) =
[vectora(point_num_limited,:,frame_num)'
vectorb(point_num_limited,:,frame_num)']*invundA(:,:,point_num_limited)
;
            Ea(:,:,point_num_limited,frame_num) =
((Fa(:,:,point_num_limited,frame_num)'*Fa(:,:,point_num_limited,frame_n
um))-eye(2))/2;    % Eq 3.7
        end
    end

    clear testfa_xx testfa_yy testfa_xy1 testfa_xy2
    for point_num_limited =1:limit_points,
        for frame_num = 1:frames,
            testfa_xx(frame_num,point_num_limited) =
Fa(1,1,point_num_limited,frame_num);
            testfa_yy(frame_num,point_num_limited) =
Fa(2,2,point_num_limited,frame_num);
```

```matlab
            testfa_xy1(frame_num,point_num_limited) =
Fa(1,2,point_num_limited,frame_num);
            testfa_xy2(frame_num,point_num_limited) =
Fa(2,1,point_num_limited,frame_num);
        end
    end

    clear testEa_xx testEa_yy testEa_xy1 testEa_xy2
    for point_num_limited =1:limit_points,
        for frame_num = 1:frames,
            testEa_xx(frame_num,point_num_limited) =
Ea(1,1,point_num_limited,frame_num);
            testEa_yy(frame_num,point_num_limited) =
Ea(2,2,point_num_limited,frame_num);
            testEa_xy1(frame_num,point_num_limited) =
Ea(1,2,point_num_limited,frame_num);
            testEa_xy2(frame_num,point_num_limited) =
Ea(2,1,point_num_limited,frame_num);
        end
    end

    % Script For creating principal strain and maximum shear strain.
    clear norm_p_strain_1 norm_p_strain_2 shear_p_strain_3
    for square_num = 1:limit_points
        for t=1:frames
            p_strain_1_norm(square_num,t) = (testEa_xx(t,square_num) +
testEa_yy(t,square_num))/2+sqrt(((testEa_xx(t,square_num) -
testEa_yy(t,square_num))/2)^2 + (testEa_xy1(t,square_num)/2)^2); %Eq
3.9
            p_strain_2_norm(square_num,t) = (testEa_xx(t,square_num) +
testEa_yy(t,square_num))/2-sqrt(((testEa_xx(t,square_num) -
testEa_yy(t,square_num))/2)^2 + (testEa_xy1(t,square_num)/2)^2); %Eq
3.10
            p_strain_3_shear(square_num,t) =
2*sqrt(((testEa_xx(t,square_num) - testEa_yy(t,square_num))/2)^2 +
(testEa_xy1(t,square_num)/2)^2); %Eq 3.11
        end
    end
end

% Contour box
zeros_strain_1= zeros(176,frames);
zeros_strain_1(001:016,:)= vertcat(zeros(6,frames),
p_strain_1_norm(71:75,:),
zeros(5,frames));
zeros_strain_1(017:032,:)= vertcat(zeros(4,frames),
p_strain_1_norm(76:84,:),
zeros(3,frames));
zeros_strain_1(033:048,:)= vertcat(zeros(3,frames),
p_strain_1_norm(1:10,:),    p_strain_1_norm(85,:),
zeros(2,frames));
zeros_strain_1(049:064,:)= vertcat(zeros(2,frames),
p_strain_1_norm(86,:),      p_strain_1_norm(11:20,:),
p_strain_1_norm(87:88,:),   zeros(1,frames));
```

```
zeros_strain_1(065:080,:)= vertcat(zeros(1,frames),
p_strain_1_norm(89:90,:),   p_strain_1_norm(21:30,:),
p_strain_1_norm(91:93,:)                        );
zeros_strain_1(081:096,:)= vertcat(
p_strain_1_norm(94:96,:),   p_strain_1_norm(31:40,:),
p_strain_1_norm(97:99,:)                        );
zeros_strain_1(097:112,:)= vertcat(
p_strain_1_norm(100:102,:), p_strain_1_norm(41:50,:),
p_strain_1_norm(103:105,:)                      );
zeros_strain_1(113:128,:)= vertcat(
p_strain_1_norm(106:108,:), p_strain_1_norm(51:60,:),
p_strain_1_norm(109:111,:)                      );
zeros_strain_1(129:144,:)= vertcat(zeros(2,frames),
p_strain_1_norm(112,:),     p_strain_1_norm(61:70,:),
p_strain_1_norm(113:114,:), zeros(1,frames));
zeros_strain_1(145:160,:)= vertcat(zeros(6,frames),
p_strain_1_norm(115:117,:), zeros(3,frames),
p_strain_1_norm(118:119,:), zeros(2,frames));
zeros_strain_1(161:176,:)= vertcat(zeros(6,frames),
p_strain_1_norm(120:121,:), zeros(8,frames)
);


zeros_strain_2= zeros(176,frames);
zeros_strain_2(001:016,:,:)= vertcat(zeros(6,frames),
p_strain_2_norm(71:75,:),
zeros(5,frames));
zeros_strain_2(017:032,:,:)= vertcat(zeros(4,frames),
p_strain_2_norm(76:84,:),
zeros(3,frames));
zeros_strain_2(033:048,:,:)= vertcat(zeros(3,frames),
p_strain_2_norm(1:10,:),    p_strain_2_norm(85,:),
zeros(2,frames));
zeros_strain_2(049:064,:,:)= vertcat(zeros(2,frames),
p_strain_2_norm(86,:),      p_strain_2_norm(11:20,:),
p_strain_2_norm(87:88,:),   zeros(1,frames));
zeros_strain_2(065:080,:,:)= vertcat(zeros(1,frames),
p_strain_2_norm(89:90,:),   p_strain_2_norm(21:30,:),
p_strain_2_norm(91:93,:)                        );
zeros_strain_2(081:096,:,:)= vertcat(
p_strain_2_norm(94:96,:),   p_strain_2_norm(31:40,:),
p_strain_2_norm(97:99,:)                        );
zeros_strain_2(097:112,:,:)= vertcat(
p_strain_2_norm(100:102,:), p_strain_2_norm(41:50,:),
p_strain_2_norm(103:105,:)                      );
zeros_strain_2(113:128,:,:)= vertcat(
p_strain_2_norm(106:108,:), p_strain_2_norm(51:60,:),
p_strain_2_norm(109:111,:)                      );
zeros_strain_2(129:144,:,:)= vertcat(zeros(2,frames),
p_strain_2_norm(112,:),     p_strain_2_norm(61:70,:),
p_strain_2_norm(113:114,:), zeros(1,frames));
zeros_strain_2(145:160,:,:)= vertcat(zeros(6,frames),
p_strain_2_norm(115:117,:), zeros(3,frames),
p_strain_2_norm(118:119,:), zeros(2,frames));
zeros_strain_2(161:176,:,:)= vertcat(zeros(6,frames),
p_strain_2_norm(120:121,:), zeros(8,frames)
);
```

```
zeros_strain_3= zeros(176,frames);
zeros_strain_3(001:016,:,:)= vertcat(zeros(6,frames),
p_strain_3_shear(71:75,:),
zeros(5,frames));
zeros_strain_3(017:032,:,:)= vertcat(zeros(4,frames),
p_strain_3_shear(76:84,:),
zeros(3,frames));
zeros_strain_3(033:048,:,:)= vertcat(zeros(3,frames),
p_strain_3_shear(1:10,:),    p_strain_3_shear(85,:),
zeros(2,frames));
zeros_strain_3(049:064,:,:)= vertcat(zeros(2,frames),
p_strain_3_shear(86,:),      p_strain_3_shear(11:20,:),
p_strain_3_shear(87:88,:),   zeros(1,frames));
zeros_strain_3(065:080,:,:)= vertcat(zeros(1,frames),
p_strain_3_shear(89:90,:),   p_strain_3_shear(21:30,:),
p_strain_3_shear(91:93,:)                    );
zeros_strain_3(081:096,:,:)= vertcat(
p_strain_3_shear(94:96,:),   p_strain_3_shear(31:40,:),
p_strain_3_shear(97:99,:)                    );
zeros_strain_3(097:112,:,:)= vertcat(
p_strain_3_shear(100:102,:), p_strain_3_shear(41:50,:),
p_strain_3_shear(103:105,:)                  );
zeros_strain_3(113:128,:,:)= vertcat(
p_strain_3_shear(106:108,:), p_strain_3_shear(51:60,:),
p_strain_3_shear(109:111,:)                   );
zeros_strain_3(129:144,:,:)= vertcat(zeros(2,frames),
p_strain_3_shear(112,:),     p_strain_3_shear(61:70,:),
p_strain_3_shear(113:114,:), zeros(1,frames));
zeros_strain_3(145:160,:,:)= vertcat(zeros(6,frames),
p_strain_3_shear(115:117,:), zeros(3,frames),
p_strain_3_shear(118:119,:), zeros(2,frames));
zeros_strain_3(161:176,:,:)= vertcat(zeros(6,frames),
p_strain_3_shear(120:121,:), zeros(8,frames)
);

for frame_num=1:frames

grid_strain_1(:,:,frame_num)=vec2mat(zeros_strain_1(:,frame_num),15);

grid_strain_2(:,:,frame_num)=vec2mat(zeros_strain_2(:,frame_num),15);

grid_strain_3(:,:,frame_num)=vec2mat(zeros_strain_3(:,frame_num),15);
end

extras=[1,11; 2,14; 3,15; 4,15; 5,15; 6,15; 7,15; 8,15; 9,15; 9,8;
10,8; 11,8; 11,3;  12,2; 12,3];
grid_strain_1_cut=grid_strain_1;

for frame_num=1:frames
    for extra_num=1:length(extras)

grid_strain_1_cut(extras(extra_num,1),extras(extra_num,2),frame_num)=0;
    end
end
grid_strain_1(:,:,42)
```

```matlab
grid_strain_1_cut(:,:,42)

for i=1:frames
    %contourf(flipud(grid_strain_1(:,:,i)));
    %imagesc(flipud(grid_strain_1(:,:,i)));
    imagesc(grid_strain_2(:,:,i));

    grid on
    colormap jet
    caxis([-.2 0.3])
    colorbar
    shg
    pause



    ax=gca;
    ax.Visible= 'off';
    set(gca,'position',[0 0 1 1],'units','normalized')
end

clear C x y vx vy D
i=47;
C= rgb2gray(imread('C:\Users\BlastLab\Documents\MATLAB\untitled.tif'));
% test image
[x, y] = meshgrid(1:size(C,2), 1:size(C,1));

% generate synthetic test data, for experimenting
vx = 0.1*y;    % an arbitrary flow field, in this case
vy = 0.5*x;    % representing shear

% compute the warped image - the subtractions are because we're
specifying
% where in the original image each pixel in the new image comes from
D =
interp2(pointloc_vector_a_all(:,2),pointloc_vector_b_all(:,2),double(C)
, x-vx, y-vy);

% display the result
imagesc(D);
grid_strain_2(:,1,1)



clear all
dirdata00=dir('C:\Users\BlastLab\Desktop\Abdus\ChenStuff\10\*');dirdata
00=dirdata00(3:end);
anchor_data01 =
xlsread(['C:\Users\BlastLab\Desktop\Abdus\ChenStuff\10\'
dirdata00(1).name '\2Dtracking_inches.xlsx'],'C24:D224');
anchor_data02 =
xlsread(['C:\Users\BlastLab\Desktop\Abdus\ChenStuff\10\'
dirdata00(1).name '\2Dtracking_inches.xlsx'],'U24:V224');
anchor_data03 =
xlsread(['C:\Users\BlastLab\Desktop\Abdus\ChenStuff\10\'
dirdata00(1).name '\2Dtracking_inches.xlsx'],'DS24:DT224');
```

```matlab
anchor_data04 =
xlsread(['C:\Users\BlastLab\Desktop\Abdus\ChenStuff\10\'
dirdata00(1).name '\2Dtracking_inches.xlsx'],'EK24:EL224');


x1= anchor_data03(:,1)./2;
x2= anchor_data02(:,1)./2;
y1= anchor_data01(:,2)./2;
y2= anchor_data04(:,2)./2;


vid00=VideoReader(['C:\Users\BlastLab\Desktop\Abdus\ChenStuff\10\'
dirdata00(1).name '\' dirdata00(1).name '.avi']);
for i=1:length(x1)
    vid01=mat2gray(vid00.read(i));
    vid02=imresize(vid01,0.5);   %makes it 512x512
    imshow(vid02)


im00=imread(['C:\Users\BlastLab\Desktop\Abdus\20160531\20160531_1_9cm_c
rown_C001H001S0001\strainmaps\strain03\20160531_1_9cm_crown_03'
num2str(sprintf('%03d',i)) '.png']);
    im01=imresize(im00,0.15);
    im02=imrotate(im01,-36.3411);
    im03=im02;
    hold on

    TrackingContour=image([x1(i) x2(i)],[y1(i) y2(i)],im03);
    set(TrackingContour,'AlphaData',0.5);
    pause
    %set(TrackingContour,'Visible','off')
    hold off
end



clear all

%%
dir_20=dir('C:\Users\BlastLab\Desktop\Abdus\20160731_ReDo\20\2016*');
dir_20={dir_20.name};
sub_num=10;
load('C:\Users\BlastLab\Desktop\Abdus\AnalyzedStuff\data_most.mat')
plot(save_StrainAll_PostImp_Renum_NoBad_NoEdges_20(20,:,3,sub_num),'k',
'LineWidth',4)
%axis([0 40 -.3 .4])
set(gca,'FontWeight','bold','FontSize',20)
xlabel ('Time (ms)','FontWeight','bold','FontSize',30); ylabel('?
Strain','FontWeight','bold','FontSize',30)
grid on
shg


%%
dir_10=dir('C:\Users\BlastLab\Desktop\Abdus\20160731_ReDo\10\2016*');
dir_20=dir('C:\Users\BlastLab\Desktop\Abdus\20160731_ReDo\20\2016*');
dir_10={dir_10.name};
```

```matlab
dir_20={dir_20.name};
sub_num=1;
load('C:\Users\BlastLab\Desktop\Abdus\AnalyzedStuff\data_most.mat')
hold on
plot(save_StrainAll_PostImp_Renum_NoBad_NoEdges_20(20,:,1,sub_num),'cya
n','LineWidth',4)
plot(save_StrainAll_PostImp_Renum_NoBad_NoEdges_20(20,:,2,sub_num),'cya
n','LineWidth',4)
plot(save_StrainAll_PostImp_Renum_NoBad_NoEdges_20(20,:,3,sub_num),'gre
en','LineWidth',4)
hold off
axis([0 40 -.3 .4])
set(gca,'FontWeight','bold','FontSize',20)
xlabel ('Time (ms)','FontWeight','bold','FontSize',30);
ylabel('Strain','FontWeight','bold','FontSize',30)
legend('?_{1}','?_{2}','?_{max}')
grid on
shg

%p90
figure()
plot(save_StrainAll_PostImp_Renum_NoBad_NoEdges_20(90,:,1,sub_num),'red
','LineWidth',4)
hold on
plot(save_StrainAll_PostImp_Renum_NoBad_NoEdges_20(90,:,2,sub_num),'cya
n','LineWidth',4)
plot(save_StrainAll_PostImp_Renum_NoBad_NoEdges_20(90,:,3,sub_num),'gre
en','LineWidth',4)
hold off
axis([0 40 -.3 .4])
set(gca,'FontWeight','bold','FontSize',20)
xlabel ('Time (ms)','FontWeight','bold','FontSize',30);
ylabel('Strain','FontWeight','bold','FontSize',30)
legend('?_{1}','?_{2}','?_{max}')
grid on
shg

%% Front
sub_num=4;

% p1
figure()
plot(save_StrainAll_PostImp_Renum_NoBad_NoEdges_20(1,:,1,sub_num),'red'
,'LineWidth',4)
hold on
plot(save_StrainAll_PostImp_Renum_NoBad_NoEdges_20(1,:,2,sub_num),'cyan
','LineWidth',4)
plot(save_StrainAll_PostImp_Renum_NoBad_NoEdges_20(1,:,3,sub_num),'gree
n','LineWidth',4)
hold off
axis([0 40 -.3 .4])
set(gca,'FontWeight','bold','FontSize',20)
xlabel ('Time (ms)','FontWeight','bold','FontSize',30);
ylabel('Strain','FontWeight','bold','FontSize',30)
legend('?_{1}','?_{2}','?_{max}')
grid on
```

```matlab
shg

% p20
figure()
plot(save_StrainAll_PostImp_Renum_NoBad_NoEdges_20(20,:,1,sub_num),'red
','LineWidth',4)
hold on
plot(save_StrainAll_PostImp_Renum_NoBad_NoEdges_20(20,:,2,sub_num),'cya
n','LineWidth',4)
plot(save_StrainAll_PostImp_Renum_NoBad_NoEdges_20(20,:,3,sub_num),'gre
en','LineWidth',4)
hold off
axis([0 40 -.3 .4])
set(gca,'FontWeight','bold','FontSize',20)
xlabel ('Time (ms)','FontWeight','bold','FontSize',30);
ylabel('Strain','FontWeight','bold','FontSize',30)
legend('?_{1}','?_{2}','?_{max}')
grid on
shg

% p90
figure()
plot(save_StrainAll_PostImp_Renum_NoBad_NoEdges_20(90,:,1,sub_num),'red
','LineWidth',4)
hold on
plot(save_StrainAll_PostImp_Renum_NoBad_NoEdges_20(90,:,2,sub_num),'cya
n','LineWidth',4)
plot(save_StrainAll_PostImp_Renum_NoBad_NoEdges_20(90,:,3,sub_num),'gre
en','LineWidth',4)
hold off
axis([0 40 -.3 .4])
set(gca,'FontWeight','bold','FontSize',20)
xlabel ('Time (ms)','FontWeight','bold','FontSize',30);
ylabel('Strain','FontWeight','bold','FontSize',30)
legend('?','?_{2}','?_{max}')
grid on
shg

%% Calculate strain rates
dummy_10=permute(save_StrainAll_PostImp_Renum_NoBad_NoEdges_10,[2,1,3,4
]);
dummy_20=permute(save_StrainAll_PostImp_Renum_NoBad_NoEdges_20,[2,1,3,4
]);
diff_10=diff(dummy_10);
diff_20=diff(dummy_20);


clear dstrainrate10
for dsub=1:24
    for dstrain=1:3
        for dloc=1:111

tstrain10=squeeze(save_StrainAll_PostImp_Renum_NoBad_NoEdges_10(dloc,:,
dstrain,dsub));
            if dstrain==2
                [~,dmaxframe10]=min(tstrain10);
```

```matlab
            else
                [~,dmaxframe10]=max(tstrain10);
            end
            ddstrainrate10=diff_10(1:dmaxframe10-1,dloc,dstrain,dsub);
%Subtract 1 bc of diff; ex. max is @ frame 2, rate is @ diff(1)
            if isempty(ddstrainrate10)==1 % if its a zero series,
                dstrainrate10(dloc,dstrain,dsub)=0; % set it to zero
            elseif dstrain~=2 && isempty(ddstrainrate10)==0 &&
isempty(find(ddstrainrate10<0)) ==1 % if there are no (-) strain rates
in the nonzero tension/shear series,

dstrainrate10(dloc,dstrain,dsub)=mean(ddstrainrate10); % average it all
            elseif dstrain==2 && isempty(ddstrainrate10)==0 &&
isempty(find(ddstrainrate10>0)) ==1 % if there are  no (+) strain rates
in the nonzero series (for compression),

dstrainrate10(dloc,dstrain,dsub)=mean(ddstrainrate10); % average it all
            elseif dstrain~=2 && isempty(ddstrainrate10)==0 &&
isempty(find(ddstrainrate10<0)) ==0 %if there are (-) values in the
nonzero tension/shear series,
                dummy1=max(find(ddstrainrate10<0))+1; %Include only
positive strain rates

dstrainrate10(dloc,dstrain,dsub)=mean(ddstrainrate10(dummy1:end));
            elseif dstrain==2 && isempty(ddstrainrate10)==0 &&
isempty(find(ddstrainrate10>0)) ==0 %if there are (+) values in the
nonzero compression series,
                dummy1=max(find(ddstrainrate10>0))+1; %Include only
negative strain rates

dstrainrate10(dloc,dstrain,dsub)=mean(ddstrainrate10(dummy1:end));
            end
        end
    end
end
dir10crown=find(~cellfun(@isempty,strfind(dir_10,'_25cm_crown')));
dir10front=find(~cellfun(@isempty,strfind(dir_10,'_25cm_front')));
gstrainrate10=mean(dstrainrate10,3);
gstrainrate10_crown5=mean(dstrainrate10(:,:,dir10crown),3);
gstrainrate10_front5=mean(dstrainrate10(:,:,dir10front),3);

clear dstrainrate20
for dsub=1:24
    for dstrain=1:3
        for dloc=1:126

tstrain20=squeeze(save_StrainAll_PostImp_Renum_NoBad_NoEdges_20(dloc,:,
dstrain,dsub));
            if dstrain==2
                [~,dmaxframe20]=min(tstrain20);
            else
                [~,dmaxframe20]=max(tstrain20);
            end
            ddstrainrate20=diff_20(1:dmaxframe20-1,dloc,dstrain,dsub);
%Subtract 1 bc of diff; ex. max is @ frame 2, rate is @ diff(1)
            if isempty(ddstrainrate20)==1 % if its a zero series,
                dstrainrate20(dloc,dstrain,dsub)=0; % set it to zero
```

```matlab
            elseif dstrain~=2 && isempty(ddstrainrate20)==0 &&
isempty(find(ddstrainrate20<0)) ==1 % if there are no (-) strain rates
in the nonzero tension/shear series,

dstrainrate20(dloc,dstrain,dsub)=mean(ddstrainrate20); % average it all
            elseif dstrain==2 && isempty(ddstrainrate20)==0 &&
isempty(find(ddstrainrate20>0)) ==1 % if there are  no (+) strain rates
in the nonzero series (for compression),

dstrainrate20(dloc,dstrain,dsub)=mean(ddstrainrate20); % average it all
            elseif dstrain~=2 && isempty(ddstrainrate20)==0 &&
isempty(find(ddstrainrate20<0)) ==0 %if there are (-) values in the
nonzero tension/shear series,
                dummy1=max(find(ddstrainrate20<0))+1; %Include only
positive strain rates

dstrainrate20(dloc,dstrain,dsub)=mean(ddstrainrate20(dummy1:end));
            elseif dstrain==2 && isempty(ddstrainrate20)==0 &&
isempty(find(ddstrainrate20>0)) ==0 %if there are (+) values in the
nonzero compression series,
                dummy1=max(find(ddstrainrate20>0))+1; %Include only
negative strain rates

dstrainrate20(dloc,dstrain,dsub)=mean(ddstrainrate20(dummy1:end));
            end
        end
    end
end
dir20crown=find(~cellfun(@isempty,strfind(dir_20,'_25cm_crown')));
dir20front=find(~cellfun(@isempty,strfind(dir_20,'_25cm_front')));
gstrainrate20=mean(dstrainrate20,3);
gstrainrate20_crown5=mean(dstrainrate20(:,:,dir20crown),3);
gstrainrate20_front5=mean(dstrainrate20(:,:,dir20front),3);


clear rate_padded10 rate_padded20 im_sr10 im_sr20
for dim_num=1:3
    rate_padded10(1:135,dim_num)= vertcat([zeros(1,5),
gstrainrate10(1:5,dim_num)', zeros(1,8), gstrainrate10(6:14,dim_num)',
zeros(1,5),gstrainrate10(15:25,dim_num)', zeros(1,3),
gstrainrate10(26:38,dim_num)', zeros(1,1),
gstrainrate10(39:98,dim_num)', zeros(1,1),
gstrainrate10(099:111,dim_num)', zeros(1,1)]);
    rate_padded10crown(1:135,dim_num)= vertcat([zeros(1,5),
gstrainrate10_crown5(1:5,dim_num)', zeros(1,8),
gstrainrate10_crown5(6:14,dim_num)',
zeros(1,5),gstrainrate10_crown5(15:25,dim_num)', zeros(1,3),
gstrainrate10_crown5(26:38,dim_num)', zeros(1,1),
gstrainrate10_crown5(39:98,dim_num)', zeros(1,1),
gstrainrate10_crown5(099:111,dim_num)', zeros(1,1)]);
    rate_padded10front(1:135,dim_num)= vertcat([zeros(1,5),
gstrainrate10_front5(1:5,dim_num)', zeros(1,8),
gstrainrate10_front5(6:14,dim_num)',
zeros(1,5),gstrainrate10_front5(15:25,dim_num)', zeros(1,3),
gstrainrate10_front5(26:38,dim_num)', zeros(1,1),
```

```
gstrainrate10_front5(39:98,dim_num)', zeros(1,1),
gstrainrate10_front5(099:111,dim_num)', zeros(1,1)]);


    rate_padded20(1:165,dim_num)= vertcat([zeros(1,4),
gstrainrate20(1:8,dim_num)', zeros(1,5), gstrainrate20(9:19,dim_num)',
zeros(1,3),gstrainrate20(20:32,dim_num)', zeros(1,1),
gstrainrate20(33:46,dim_num)', zeros(1,1),
gstrainrate20(47:91,dim_num)', zeros(1,2),
gstrainrate20(092:104,dim_num)', zeros(1,4),
gstrainrate20(105:115,dim_num)', zeros(1,8),
gstrainrate20(116:121,dim_num)', zeros(1,9),
gstrainrate20(122:126,dim_num)', zeros(1,2)]);
    rate_padded20crown(1:165,dim_num)= vertcat([zeros(1,4),
gstrainrate20_crown5(1:8,dim_num)', zeros(1,5),
gstrainrate20_crown5(9:19,dim_num)',
zeros(1,3),gstrainrate20_crown5(20:32,dim_num)', zeros(1,1),
gstrainrate20_crown5(33:46,dim_num)', zeros(1,1),
gstrainrate20_crown5(47:91,dim_num)', zeros(1,2),
gstrainrate20_crown5(092:104,dim_num)', zeros(1,4),
gstrainrate20_crown5(105:115,dim_num)', zeros(1,8),
gstrainrate20_crown5(116:121,dim_num)', zeros(1,9),
gstrainrate20_crown5(122:126,dim_num)', zeros(1,2)]);
    rate_padded20front(1:165,dim_num)= vertcat([zeros(1,4),
gstrainrate20_front5(1:8,dim_num)', zeros(1,5),
gstrainrate20_front5(9:19,dim_num)',
zeros(1,3),gstrainrate20_front5(20:32,dim_num)', zeros(1,1),
gstrainrate20_front5(33:46,dim_num)', zeros(1,1),
gstrainrate20_front5(47:91,dim_num)', zeros(1,2),
gstrainrate20_front5(092:104,dim_num)', zeros(1,4),
gstrainrate20_front5(105:115,dim_num)', zeros(1,8),
gstrainrate20_front5(116:121,dim_num)', zeros(1,9),
gstrainrate20_front5(122:126,dim_num)', zeros(1,2)]);


    im_sr10(:,:,dim_num)=vec2mat(rate_padded10(:,dim_num),15);

im_sr10crown(:,:,dim_num)=vec2mat(rate_padded10crown(:,dim_num),15);

im_sr10front(:,:,dim_num)=vec2mat(rate_padded10front(:,dim_num),15);

    im_sr20(:,:,dim_num)=vec2mat(rate_padded20(:,dim_num),15);

im_sr20crown(:,:,dim_num)=vec2mat(rate_padded20crown(:,dim_num),15);

im_sr20front(:,:,dim_num)=vec2mat(rate_padded20front(:,dim_num),15);
end
figure(); imagesc(im_sr20crown(:,:,dim_num))
figure(); imagesc(im_sr20front(:,:,dim_num))

figure(); colormap(jet);
set(gcf,'units','points','position',[1,1,450,330])
contourf(flipud(im_sr20crown(:,:,1))); caxis([-.10 .15]);
set(gca,'visible','off');
figure(); colormap(jet);
set(gcf,'units','points','position',[1,1,450,330])
contourf(flipud(im_sr20crown(:,:,2))); caxis([-.10 .15]);
set(gca,'visible','off');
```

```matlab
figure(); colormap(jet);
set(gcf,'units','points','position',[1,1,450,330])
contourf(flipud(im_sr20crown(:,:,3))); caxis([-.10 .15]);
set(gca,'visible','off');
figure(); colormap(jet);
set(gcf,'units','points','position',[1,1,450,330])
contourf(flipud(im_sr20front(:,:,1))); caxis([-.10 .15]);
set(gca,'visible','off');
figure(); colormap(jet);
set(gcf,'units','points','position',[1,1,450,330])
contourf(flipud(im_sr20front(:,:,2))); caxis([-.10 .15]);
set(gca,'visible','off');
figure(); colormap(jet);
set(gcf,'units','points','position',[1,1,450,330])
contourf(flipud(im_sr20front(:,:,3))); caxis([-.10 .15]);
set(gca,'visible','off');
figure(); colormap(jet); caxis([-.10 .15]); set(gca,'visible','off');

%%
%% Looking at corr

dummy0x=find(~cellfun(@isempty,strfind(dir_10,'10%')));
dummy1x=find(~cellfun(@isempty,strfind(dir_10,'_09cm')));
dummy2x=find(~cellfun(@isempty,strfind(dir_10,'_25cm')));
dummy00x=find(~cellfun(@isempty,strfind(dir_10,'crown')));
dummy10x=find(~cellfun(@isempty,strfind(dir_10,'_09cm_crown')));
dummy20x=find(~cellfun(@isempty,strfind(dir_10,'_25cm_crown')));
dummy000x=find(~cellfun(@isempty,strfind(dir_10,'front')));
dummy100x=find(~cellfun(@isempty,strfind(dir_10,'_09cm_front')));
dummy200x=find(~cellfun(@isempty,strfind(dir_10,'_25cm_front')));
dummy0y=find(~cellfun(@isempty,strfind(dir_20,'20%')));
dummy1y=find(~cellfun(@isempty,strfind(dir_20,'_09cm')));
dummy2y=find(~cellfun(@isempty,strfind(dir_20,'_25cm')));
dummy00y=find(~cellfun(@isempty,strfind(dir_20,'crown')));
dummy10y=find(~cellfun(@isempty,strfind(dir_20,'_09cm_crown')));
dummy20y=find(~cellfun(@isempty,strfind(dir_20,'_25cm_crown')));
dummy000y=find(~cellfun(@isempty,strfind(dir_20,'front')));
dummy100y=find(~cellfun(@isempty,strfind(dir_20,'_09cm_front')));
dummy200y=find(~cellfun(@isempty,strfind(dir_20,'_25cm_front')));

corr_10=zeros(24,3);
corr_20=zeros(24,3);
corr_crownx=zeros(12,3);
corr_crowny=zeros(12,3);
corr_frontx=zeros(12,3);
corr_fronty=zeros(12,3);
corr_3mphx=zeros(12,3);
corr_5mphx=zeros(12,3);
corr_3mphy=zeros(12,3);
corr_5mphy=zeros(12,3);
p10=zeros(12,3);
p20=zeros(12,3);
pcrownx=zeros(12,3);
pcrowny=zeros(12,3);
pfrontx=zeros(12,3);
pfronty=zeros(12,3);
```

```matlab
p3mphx=zeros(12,3);
p3mphy=zeros(12,3);
p5mphx=zeros(12,3);
p5mphy=zeros(12,3);


nz10=find(save_StrainAll_PostImp_Renum_NoBad_NoEdges_Maxes_10(:,1,1));
nz20=find(save_StrainAll_PostImp_Renum_NoBad_NoEdges_Maxes_20(:,1,1));


for dir_num=1:24
    for strain_num=1:3
        [corr_10(dir_num,strain_num) p10(dir_num,strain_num)]=
corr(save_StrainAll_PostImp_Renum_NoBad_NoEdges_Maxes_10(nz10,strain_nu
m,dir_num),dstrainrate10(nz10,strain_num,dir_num),'type','Spearman');
        [corr_20(dir_num,strain_num) p20(dir_num,strain_num)]=
corr(save_StrainAll_PostImp_Renum_NoBad_NoEdges_Maxes_20(nz20,strain_nu
m,dir_num),dstrainrate20(nz20,strain_num,dir_num),'type','Spearman');
    end
end

for dir_num=1:12
    for strain_num=1:3
        [corr_crownx(dir_num,strain_num) pcrownx(dir_num,strain_num)]=
corr(save_StrainAll_PostImp_Renum_NoBad_NoEdges_Maxes_10(nz10,strain_nu
m,dummy00x(dir_num)),dstrainrate10(nz10,strain_num,dummy00x(dir_num)),'
type','Spearman');
        [corr_crowny(dir_num,strain_num) pcrowny(dir_num,strain_num)]=
corr(save_StrainAll_PostImp_Renum_NoBad_NoEdges_Maxes_20(nz20,strain_nu
m,dummy00y(dir_num)),dstrainrate20(nz20,strain_num,dummy00y(dir_num)),'
type','Spearman');
        [corr_frontx(dir_num,strain_num) pfrontx(dir_num,strain_num)]=
corr(save_StrainAll_PostImp_Renum_NoBad_NoEdges_Maxes_10(nz10,strain_nu
m,dummy000x(dir_num)),dstrainrate10(nz10,strain_num,dummy000x(dir_num))
,'type','Spearman');
        [corr_fronty(dir_num,strain_num) pfronty(dir_num,strain_num)]=
corr(save_StrainAll_PostImp_Renum_NoBad_NoEdges_Maxes_20(nz20,strain_nu
m,dummy000y(dir_num)),dstrainrate20(nz20,strain_num,dummy000y(dir_num))
,'type','Spearman');
        [corr_3mphx(dir_num,strain_num) p3mphx(dir_num,strain_num)]=
corr(save_StrainAll_PostImp_Renum_NoBad_NoEdges_Maxes_10(nz10,strain_nu
m,dummy1x(dir_num)),dstrainrate10(nz10,strain_num,dummy1x(dir_num)),'ty
pe','Spearman');
        [corr_3mphy(dir_num,strain_num) p3mphy(dir_num,strain_num)]=
corr(save_StrainAll_PostImp_Renum_NoBad_NoEdges_Maxes_20(nz20,strain_nu
m,dummy1y(dir_num)),dstrainrate20(nz20,strain_num,dummy1y(dir_num)),'ty
pe','Spearman');
        [corr_5mphx(dir_num,strain_num) p5mphx(dir_num,strain_num)]=
corr(save_StrainAll_PostImp_Renum_NoBad_NoEdges_Maxes_10(nz10,strain_nu
m,dummy2x(dir_num)),dstrainrate10(nz10,strain_num,dummy2x(dir_num)),'ty
pe','Spearman');
        [corr_5mphy(dir_num,strain_num) p5mphy(dir_num,strain_num)]=
corr(save_StrainAll_PostImp_Renum_NoBad_NoEdges_Maxes_20(nz20,strain_nu
m,dummy2y(dir_num)),dstrainrate20(nz20,strain_num,dummy2y(dir_num)),'ty
pe','Spearman');
    end
end
```

```matlab
for dir_num=1:24
    for strain_num=1:3
        [corr_10(dir_num,strain_num) p10(dir_num,strain_num)]=
corr(save_StrainAll_PostImp_Renum_NoBad_NoEdges_Maxes_10(nz10,strain_nu
m,dir_num),dstrainrate10(nz10,strain_num,dir_num),'type','Pearson');
        [corr_20(dir_num,strain_num) p20(dir_num,strain_num)]=
,'type','Pearson');
    end
end
for dir_num=1:12
    for strain_num=1:3
        [corr_crownx(dir_num,strain_num) pcrownx(dir_num,strain_num)]=
corr(save_StrainAll_PostImp_Renum_NoBad_NoEdges_Maxes_10(nz10,strain_nu
m,dummy00x(dir_num)),dstrainrate10(nz10,strain_num,dummy00x(dir_num)),'
type','Pearson');
        [corr_crowny(dir_num,strain_num) pcrowny(dir_num,strain_num)]=
corr(save_StrainAll_PostImp_Renum_NoBad_NoEdges_Maxes_20(nz20,strain_nu
m,dummy00y(dir_num)),dstrainrate20(nz20,strain_num,dummy00y(dir_num)),'
type','Pearson');
        [corr_frontx(dir_num,strain_num) pfrontx(dir_num,strain_num)]=
corr(save_StrainAll_PostImp_Renum_NoBad_NoEdges_Maxes_10(nz10,strain_nu
m,dummy000x(dir_num)),dstrainrate10(nz10,strain_num,dummy000x(dir_num))
,'type','Pearson');
        [corr_fronty(dir_num,strain_num) pfronty(dir_num,strain_num)]=
corr(save_StrainAll_PostImp_Renum_NoBad_NoEdges_Maxes_20(nz20,strain_nu
m,dummy000y(dir_num)),dstrainrate20(nz20,strain_num,dummy000y(dir_num))
,'type','Pearson');
        [corr_3mphx(dir_num,strain_num) p3mphx(dir_num,strain_num)]=
corr(save_StrainAll_PostImp_Renum_NoBad_NoEdges_Maxes_10(nz10,strain_nu
m,dummy1x(dir_num)),dstrainrate10(nz10,strain_num,dummy1x(dir_num)),'ty
pe','Pearson');
        [corr_3mphy(dir_num,strain_num) p3mphy(dir_num,strain_num)]=
corr(save_StrainAll_PostImp_Renum_NoBad_NoEdges_Maxes_20(nz20,strain_nu
m,dummy1y(dir_num)),dstrainrate20(nz20,strain_num,dummy1y(dir_num)),'ty
pe','Pearson');
        [corr_5mphx(dir_num,strain_num) p5mphx(dir_num,strain_num)]=
corr(save_StrainAll_PostImp_Renum_NoBad_NoEdges_Maxes_10(nz10,strain_nu
m,dummy2x(dir_num)),dstrainrate10(nz10,strain_num,dummy2x(dir_num)),'ty
pe','Pearson');
        [corr_5mphy(dir_num,strain_num) p5mphy(dir_num,strain_num)]=
corr(save_StrainAll_PostImp_Renum_NoBad_NoEdges_Maxes_20(nz20,strain_nu
m,dummy2y(dir_num)),dstrainrate20(nz20,strain_num,dummy2y(dir_num)),'ty
pe','Pearson');
    end
end

corr_table=[mean(corr_10)
mean(corr_20)
mean(corr_crownx)
mean(corr_crowny)
mean(corr_frontx)
mean(corr_fronty)
mean(corr_3mphx)
mean(corr_3mphy)
mean(corr_5mphx)
```

```
mean(corr_5mphy)];

corr_table20 = [mean(corr_20); mean(corr_crowny); mean(corr_fronty);
mean(corr_3mphy); mean(corr_3mphy)];
imagesc(corr_table20); colormap(flipud(gray)); caxis([0 1]);
set(gca,'visible','off'); shg

mean(corr_crowny);
mean(corr_fronty);
mean(corr_3mphy);
mean(corr_3mphy)])


mean(p10)
mean(p20)

test1=squeeze(save_StrainAll_PostImp_Renum_NoBad_NoEdges_Maxes_20(nz20,
3,:));
test2=squeeze(dstrainrate20(nz20,3,:));
plot(test1(:,1),test2(:,1),'o')
hold on
for dsub=2:12
    plot(test1(:,dummy00y(dsub)),test2(:,dummy00y(dsub)),'o')
end
hold off
axis([0 0.5 0 0.25])
set(gca,'FontWeight','bold','FontSize',20)
set(gcf,'units','points','position',[1,1,1000,500])

% %%
%
dummy_10=permute(save_StrainAll_PostImp_Renum_NoBad_NoEdges_10,[2,1,3,4
]);
%
dummy_20=permute(save_StrainAll_PostImp_Renum_NoBad_NoEdges_20,[2,1,3,4
]);
% diff_10=diff(dummy_10);
% diff_20=diff(dummy_20);
% [test, testloc]=max(diff_20,[],1);
% test=squeeze(test);
% testloc=squeeze(testloc);
% [test2,testloc2]=max(test,[],1);
% test2=squeeze(test2);
% testloc2=squeeze(testloc2);
% subplot(3,1,1)
% plot(save_StrainAll_PostImp_Renum_NoBad_NoEdges_20(1,:,3,4))
% axis([0 77 -.1 .55])
% subplot(3,1,2)
% plot(diff_20(:,1,3,4))
% axis([0 77 -.1 .55])
%
% figure()
% subplot(3,1,1)
% plot(save_StrainAll_PostImp_Renum_NoBad_NoEdges_20(1,:,1,4))
% subplot(3,1,2)
% plot(save_StrainAll_PostImp_Renum_NoBad_NoEdges_20(1,:,2,4))
```

```matlab
% subplot(3,1,3)
% plot(save_StrainAll_PostImp_Renum_NoBad_NoEdges_20(1,:,3,4))

clear all
load('C:\Users\BlastLab\Desktop\Abdus\AnalyzedStuff\data_most.mat')

dirdata00=dir('C:\Users\BlastLab\Desktop\Abdus\20160731_ReDo\20\*');dir
data00=dirdata00(3:end);

anchor_data01(:,1) =
xlsread('C:\Users\BlastLab\Desktop\Abdus\20160731_ReDo\20\20160406_04_2
5cm_crown_20%_C001H001S0001\2Dtracking_inches.xlsx','BO24:BO344');
anchor_data01(:,2) =
xlsread('C:\Users\BlastLab\Desktop\Abdus\20160731_ReDo\20\20160406_04_2
5cm_crown_20%_C001H001S0001\2Dtracking_inches.xlsx','D24:D344');
anchor_data02(:,1) =
xlsread('C:\Users\BlastLab\Desktop\Abdus\20160731_ReDo\20\20160406_04_2
5cm_crown_20%_C001H001S0001\2Dtracking_inches.xlsx','DS24:DS344');
anchor_data02(:,2) =
xlsread('C:\Users\BlastLab\Desktop\Abdus\20160731_ReDo\20\20160406_04_2
5cm_crown_20%_C001H001S0001\2Dtracking_inches.xlsx','R24:R344');
anchor_data03(:,1) =
xlsread('C:\Users\BlastLab\Desktop\Abdus\20160731_ReDo\20\20160406_04_2
5cm_crown_20%_C001H001S0001\2Dtracking_inches.xlsx','EY24:EY344');
anchor_data03(:,2) =
xlsread('C:\Users\BlastLab\Desktop\Abdus\20160731_ReDo\20\20160406_04_2
5cm_crown_20%_C001H001S0001\2Dtracking_inches.xlsx','IL24:IL344');
anchor_data04(:,1) =
xlsread('C:\Users\BlastLab\Desktop\Abdus\20160731_ReDo\20\20160406_04_2
5cm_crown_20%_C001H001S0001\2Dtracking_inches.xlsx','IS24:IS344');
anchor_data04(:,2) =
xlsread('C:\Users\BlastLab\Desktop\Abdus\20160731_ReDo\20\20160406_04_2
5cm_crown_20%_C001H001S0001\2Dtracking_inches.xlsx','HX24:HX344');
x1= anchor_data03(:,1)./2;
x2= anchor_data02(:,1)./2;
y1= anchor_data01(:,2)./2;
y2= anchor_data04(:,2)./2;

dirdata01=dir(['C:\Users\BlastLab\Desktop\Abdus\20160731_ReDo\20\201604
06_04_25cm_crown_20%_C001H001S0001\20160406_drop4_C001H001S0001.avi']);
writerObj = VideoWriter('out1.avi'); % Name it.
writerObj.FrameRate = 10; % How many frames per second.
open(writerObj);


quantity_points= 126;
clear coord_xy
for i = 2:2:2*quantity_points
    coord_xy(i/2,:,:)= (anchor_data01(:,(i-1):i)').*0.5;   % xy,#frames
end

vid00=VideoReader('C:\Users\BlastLab\Desktop\Abdus\20160731_ReDo\20\201
60406_04_25cm_crown_20%_C001H001S0001\20160406_drop4_C001H001S0001.avi'
);
dummy_grid=zeros(11,15);
```

```matlab
clear strain_padded20 shapedstrain_padded20
for dim_num=1:3
    for
dtime=1:length(save_StrainAll_PostImp_Renum_NoBad_NoEdges_20(1,:,1,7))
    strain_padded20(1:165,dtime,dim_num)= vertcat([zeros(1,4),
save_StrainAll_PostImp_Renum_NoBad_NoEdges_20(1:8,dtime,dim_num,7)',
zeros(1,5),
save_StrainAll_PostImp_Renum_NoBad_NoEdges_20(9:19,dtime,dim_num,7)',
zeros(1,3),save_StrainAll_PostImp_Renum_NoBad_NoEdges_20(20:32,dtime,di
m_num,7)', zeros(1,1),
save_StrainAll_PostImp_Renum_NoBad_NoEdges_20(33:46,dtime,dim_num,7)',
zeros(1,1),
save_StrainAll_PostImp_Renum_NoBad_NoEdges_20(47:91,dtime,dim_num,7)',
zeros(1,2),
save_StrainAll_PostImp_Renum_NoBad_NoEdges_20(092:104,dtime,dim_num,7)'
, zeros(1,4),
save_StrainAll_PostImp_Renum_NoBad_NoEdges_20(105:115,dtime,dim_num,7)'
, zeros(1,8),
save_StrainAll_PostImp_Renum_NoBad_NoEdges_20(116:121,dtime,dim_num,7)'
, zeros(1,9),
save_StrainAll_PostImp_Renum_NoBad_NoEdges_20(122:126,dtime,dim_num,7)'
, zeros(1,2)]);

    shapedstrain_padded20(:,:,dtime,dim_num)=vec2mat(strain_padded20(1:165,
dtime,dim_num),15);
    end
end

% for dtime=1:77
%     contourf(flipud(shapedstrain_padded20(:,:,dtime,3)))
%     colormap jet
%     caxis([0 .5])
%     set(gca,'visible','off');
%     set(gca,'position',[0 0 1 1],'units','normalized'),shg
%     saveas(gcf,['C:\Users\BlastLab\Documents\MATLAB\test\strain3_'
num2str(dtime,'%0.3d') '.png'])
% end

for x=1:201
    vid01=mat2gray(vid00.read(x));

    contourf(anchor_data01_x,anchor_data01_y,shapedstrain_padded20,[0
0.1 0.2 0.3 0.4 0.5 0.6])

    vid02=vid01;
end
imshow(vid02)


hold on

hold off

backg=ones(100,100);
```

```
test01=rand(3,3);
testcoord(:,:,1)=[1 2 3; 1 2 3; 1 2 3].*10;
testcoord(:,:,2)=[3 3 3; 2 2 2; 1 1 1].*10;
testcoord_xcenter=testcoord(:,2,1);
testcoord_ycenter=testcoord(:,2,2);
center = repmat([testcoord_xcenter; testcoord_ycenter], 1,
length(testcoord(:,:,1)));
theta = pi/3;
R = [cos(theta) -sin(theta); sin(theta) cos(theta)];
s = v - center;
so = R*s;
vo = so + center;

imagesc(backg)
hold on
contourf(testcoord(:,:,1),testcoord(:,:,2),test01)
hold off

figure()
colormap jet
caxis([0 0.16])
```

REFERENCES

1 (2017, April). TBI: Get the Facts. *Centers for Disease Control and Prevention.* Retrieved from https://www.cdc.gov/traumaticbraininjury/get_the_facts.html

2 (2016, January). Percent Distributions of TBI-related Emergency Department Visits by Age Group and Injury Mechanism — United States, 2006–2010. *Centers for Disease Control and Prevention.* Retrieved from https://www.cdc.gov/traumaticbraininjury/data/dist_ed.html

3 (2017, February). DoD Worldwide TBI Numbers. *Defense and Veterans Brainy Injury Center.* Retrieved from http://dvbic.dcoe.mil/files/tbi-numbers/DoD-TBI-Worldwide-Totals_2000-2016_Feb-17-2017_v1.0_2017-04-06.pdf

4 (2017, February). DoD Worldwide TBI Numbers. *Defense and Veterans Brainy Injury Center.* Retrieved from http://dvbic.dcoe.mil/files/tbi-numbers/DoD-TBI-Worldwide-Totals_2016_Feb-17-2017_v1.0_2017-04-06.pdf

5 Jaslow, C. R. (1990). Mechanical properties of cranial sutures. *Journal of biomechanics*, *23*(4), 313-321.

6 Lynnerup, N., Astrup, J. G., & Sejrsen, B. (2005). Thickness of the human cranial diploe in relation to age, sex and general body build. *Head & face medicine*, *1*(1), 13.

7 Coats, B., & Margulies, S. S. (2006). Material properties of human infant skull and suture at high rates. *Journal of neurotrauma*, *23*(8), 1222-1232.

8 Schmitt, K. U., Niederer, P. F., Muser, M. H., & Walz, F. (2009). Introduction. *Trauma Biomechanics: Accidental injury in traffic and sports* (pp. 71). Berlin, Heidelberg: Springer Berlin Heidelberg.

9 Post, A., & Hoshizaki, T. B. (2012). Mechanisms of brain impact injuries and their prediction: a review. *Trauma*, *14*(4), 327-349.

10 Eppinger, R., et al. (1999). Development of improved injury criteria for the assessment of advanced automotive restraint systems–II. *National Highway Traffic Safety Administration*, 1-70.

11 Takhounts, E. G., Craig, M. J., Moorhouse, K., McFadden, J., & Hasija, V. (2013). Development of brain injury criteria (BrIC). *Stapp car crash journal*, *57*, 243.

12 Ganpule, S. G. (2013). Mechanics of blast loading on post-mortem human and surrogate heads in the study of Traumatic Brain Injury (TBI) using experimental and computational approaches. *University of Nebraska Lincoln*

13 Miao, C. (2016). Continuum mechanical analysis of space and time dependent deformation pattern of brain with blunt injury. *New Jersey Institute of Technology*